Selective Prepared Carbon Nanomaterials for Advanced Photocatalytic Application in Environmental Pollutant Treatment and Hydrogen Production

Huan Yi [a,b], Danlian Huang [a,b], Guangming Zeng [a,b,*], Cui Lai [a,b,*], Lei Qin [a,b], Min Cheng [a,b], Shujing Ye [a,b], Biao Song [a,b], Xiaoya Ren [a,b], Xueying Guo [a,b]

[a] College of Environmental Science and Engineering, Hunan University, Changsha, Hunan 410082, China

[b] Key Laboratory of Environmental Biology and Pollution Control (Hunan University), Ministry of Education, Changsha, Hunan 410082, China

---

* Corresponding author at: College of Environmental Science and Engineering, Hunan University, Changsha, Hunan 410082, China.

Tel.: +86–731– 88822754; fax: +86–731–88823701.

E-mail address: zgming@hnu.edu.cn (G.M. Zeng), laicui@hnu.edu.cn (C. Lai).

Contents

Abstract:

Highly-efficient materials and technologies for environmental pollutant treatment and hydrogen production are urgently needed in "green" 21st century. Notably, photocatalytic process over carbon nanomaterials (CNMs)-modified photocatalysts is an effective solution for these crises. CNMs (e.g., fullerenes, carbon nanotubes, graphene, carbon nanofibers, and carbon quantum dots) reveal remarkable morphological, mechanical, electrical and optical properties, which have been of significantly scientific and technological interest in photocatalysis. Until now, many efforts have been made to take advantage of these unique size- and surface-dependent properties of CNMs for photocatalytic process. In this review, we firstly summarize selective preparation of CNMs that has a great impact on their photocatalytic performance. Then we provide an updated outline of advanced photocatalytic application of CNMs in addressing both environmental pollution and hydrogen energy crisis. The difference in the role of various CNMs play in the enhancement of photocatalytic performance is also discussed. Lastly, we discuss the limitations of CNMs applied in photocatalysis or even wider fields. We hope this review will project a fast developmental path with providing a wide view of recent preparation methods, applications, prospects and challenges.

Key words: CNMs; selective preparation; photocatalysis; environmental pollutant treatment; hydrogen production.

1. Introduction

The importance of efficient pollutant treatment and hydrogen production is evident from the aggravation of energy and environmental crisis [1-7]. Photocatalysis is a low-energy technology for environmental treatment owing to the high efficiency for reduction on highly toxic contaminants and oxidation degradation on organic pollutants serving H_2O and CO_2 as the final products [8-12]. Additionally, since the photo-generation of hydrogen from water over titanium dioxide (TiO_2) photoanode under light irradiation [13], photocatalytically splitting water has been considered as a potentially significant strategy for hydrogen production [14-16]. Thus in recent decades, photocatalytic process has attracted enormous interest as an effevtive method for both environmental pollutant treatment and hydrogen production. However, most of the photocatalytic processes need to be improved because of the low quantum conversion efficiency of the absorbed light to charge carriers and high carrier recombination [17-21]. Therefore, developing efficient methods for better photocatalytic process is in demand.

Photocatalysis over carbon nanomaterials (CNMs)-modified materials is an enabling process to address environmental pollution and hydrogen energy crisis [22-24]. CNMs are one of the most promising nanomaterials today, including fullerenes, carbon nanotubes (CNTs), graphene (GR), carbon quantum dots (CQDs) and so on (Fig. 1). CNMs are classified based on the number of dimensions that not confined to the nanoscale range (<100 nm), including zero-dimensional (0D) nanoparticles, one-dimensional (1D) nanotubes, and two-dimensional (2D) nanosheets. Since they were found, CNMs have been applied in various fields, like supercapacitors [25], batteries [26], hydrogen storage [27], solar cells [28], and biomedical applications [29]. Moreover, environmental pollutants, such as heavy metal ions [30-37], organic dyes [38], colorless organics [39-45], inorganics [46] and co-pollution [47-49], apt to be effectively treated by using CNMs [50-52]. In particular, CNMs attracted enormous interest in photocatalysis field owing to the remarkable π-system formed by sp^2 hybridization. And CNMs show wonderful stability, robustness, biocompatibility, chemical inertness, high photoluminescence (PL) and conductivity [23, 53-57].

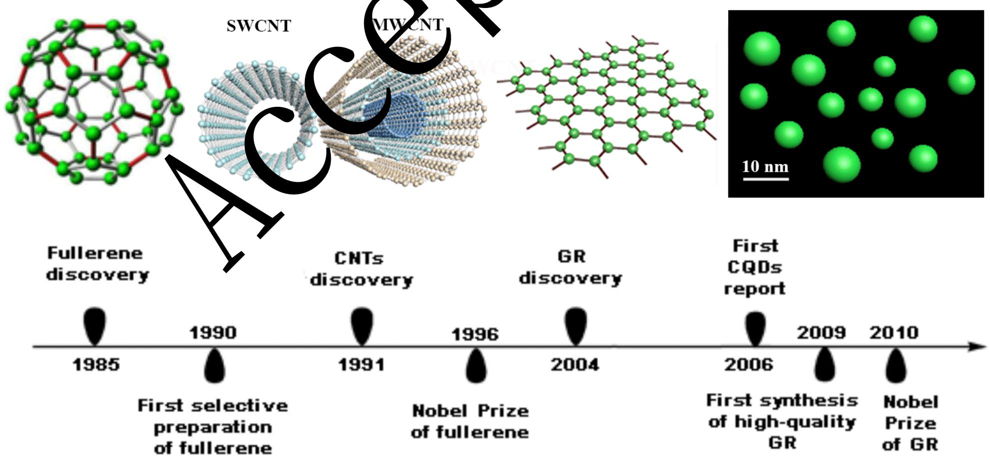

Fig. 1 Illustration of common used CNMs: fullerenes, carbon nanotubes, graphene and carbon quantum dots.

Up to now, many efforts have been made to take advantage of the unique size-, surface- and structure-dependent properties of CNMs applied in photocatalysis [58-62]. Fantastic progress has been obtained in promoting the photocatalytic performance of CNMs. CNMs are significant for their structural variability, which has a positive effect on the photocatalytic performance [63]. Further application of CNMs is initially limited by the complicated and uneconomical processes for their selective preparation with desired scale [64]. Therefore, simple and cost-effective methods for selective preparation of CNMs are rapidly in a great demand. On the other hand, application of CNMs in pollutant treatment and hydrogen production drawn increasing interest owing to the aggravation of energy and environmental crisis. Previously, π-π interactions and mechanochemistry of CNMs were discussed [63, 65], Rodrigues and Smith [66] reviewed the application of carbon-based nanomaterials for removal of chemical and biological pollutants from water, De Volder et.al. [67] summarized many commercial applications of CNTs, and Miao et.al. [68] elaborated on recent advances in catalytic application of CNTs catalysts or functionalized CNTs. However, comprehensive summary on CNMs photocatalytic applications for environmental pollutant treatment and hydrogen production and the role of π-π interactions and mechanochemistry in the photocatalytic process is still absent.

This review firstly pays attention to the reversible and sustainable selective preparation process of CNMs. Then recent advanced progress in CNMs photocatalytic applications are summarized and analyzed, along with further exploration of the role of π-π interactions and mechanochemistry in the photocatalytic process. Finally, challenges and future directions of CNMs-modified photocatalysts are discussed.

2. Selective preparation of CNMs

It was reported that structural variability positively influenced the performance of CNMs in photocatalytic process [63, 69, 70]. In detail, the photocatalytic properties are affected by the size and structure, which mainly depend on the preparation process of CNMs [64]. The primary barrier for the selective preparation is the complicated and uneconomical production process. Therefore, simple, cost-effective, and eco-friendly methods for CNMs selective preparation are urgently needed before CNMs are widely used in photocatalytic process for environmental pollutant treatment and hydrogen production.

2.1 Zero-dimensional fullerenes

Fullerenes, zero-dimensional (0D) spherical carbon cages, are simply classified based on the number of carbon atoms [71]. Fullerene C_{60} is the smallest and almost abundant fullerene, followed by C_{70} and other higher fullerenes (C_n, n > 70). Fullerenes are chemically reactive owing to the π-system, like combining with semiconductors and influencing the electron donor-acceptor system [69]. The characteristic endowed fullerenes with the capacity to be applied in the formation of novel photocatalytic materials with expected physicochemical properties [70-73]. Notably, the size of fullerenes has a great impact on fullerene properties. To further explore their size-dependent properties, many different methods have been presented to prepare fullerene molecules with desired size [74-76].

The foremost method for fullerene preparation in preparative quantities is vaporizing graphite with resistive heating in the arc plasma under low helium pressure [77]. The obtained fullerenes can keep stable in air for at least a few weeks and be used without special treatment, but with low efficient production. Soon after, a 3-phase thermal plasma process was presented for fullerene production, which realized the independent control of the input carbon rate [78]. And Churilov et.al. [79] presented a method to control the preparation process in the high-frequency arc plasma by changing the helium pressure, which illuminated the effects of arc temperature and electron concentration. Though fullerene production are mature, selective preparation of fullerene with desired size is in the early stage. For this reason, properties and application of fullerene in photocatalytic field still remain unclear.

Commonly, there are three methods used for fullerene selective preparation (Fig. 2): (i) fractional crystallization. The unit operation of fractional crystallization is divided into three steps - dissolution of crude fullerene soot extract, heating, and filtration. During the crystallization process, deposits of similar compositions from every procedure can be obtained with higher quality. To date, fractional crystallization has been a mature technology. It is simple, cost-efficient, but time-consuming because of the multiple crystallization procedures [80].

(ii) chromatographic process. Traditional chromatographic process for fullerene selective preparation often use neutral alumina as the stationary phase, and use hexane or toluene as the mobile phase [81]. The traditional process has some basic drawbacks, such as limited column loadings, time-consuming operation, and irreversible adsorption of fullerenes. Researchers in this field have been always trying to solve these drawbacks. In recent years, using metal-organic framework as the stationary phase for improving the chromatographic process has drawn increasing attention [82-84]. Current improved chromatography possesses facile operations, reversible adsorption-desorption of fullerene, low-cost and rapid manufacturing process. In addition, chromatographic technology shows the ability to achieve large-scale selective fullerene preparation [76].

(iii) selective complexation. Among these methods, selective complexation via designing appropriate molecular receptor for fullerene shows a high efficiency in selective preparation [85, 86]. Complementarity in size, shape, structure, molecular symmetry, and electronic donor-accept relying on the host-guest interaction between receptor and fullerene are crucial factors [87]. Specially, in the design of coordination metallosupramolecular receptors, different π-extended systems was utilized as molecular building blocks to improve the selectivity [64]. There are many examples of designed receptors used for fullerene selective preparation, such as the receptors synthesized by cyclodextrins [88], cycloparaphenylenes or CNTs [89], and π-extended derivatives of tetrathiafulvalene (TTF) [90]. Herein, a coordination metallosupramolecular calixar[3]arenes cage containing π-extended moieties is discussed at length [91]. It can be used for C_{60} selective preparation in a reversible way. This calixar[3]arenes cage can include C_{60} to form an adduct with 1:1 stoichiometry. Though the cavity is suitable to encapsulate C_{70} due to from the aspect of shape complementary, C_{70} is scarcely reacted with calixar[3]arenes cage. This is because the unsuitable complementarity of molecular symmetry between calixar[3]arenes cage and C_{70} [92]. Lithium cations bound to calixar[3]arenes cage can enhance the inclusion of C_{60} within the cage, whereas the bigger sodium cations can impede C_{60} encapsulation via adjusting an ellipsoidal shape when they are bound to the receptor as a substitution of lithium cations. This adjustment in the shape and size of the cage caused by cation binding contributes to fullerene C_{60} selective preparation.

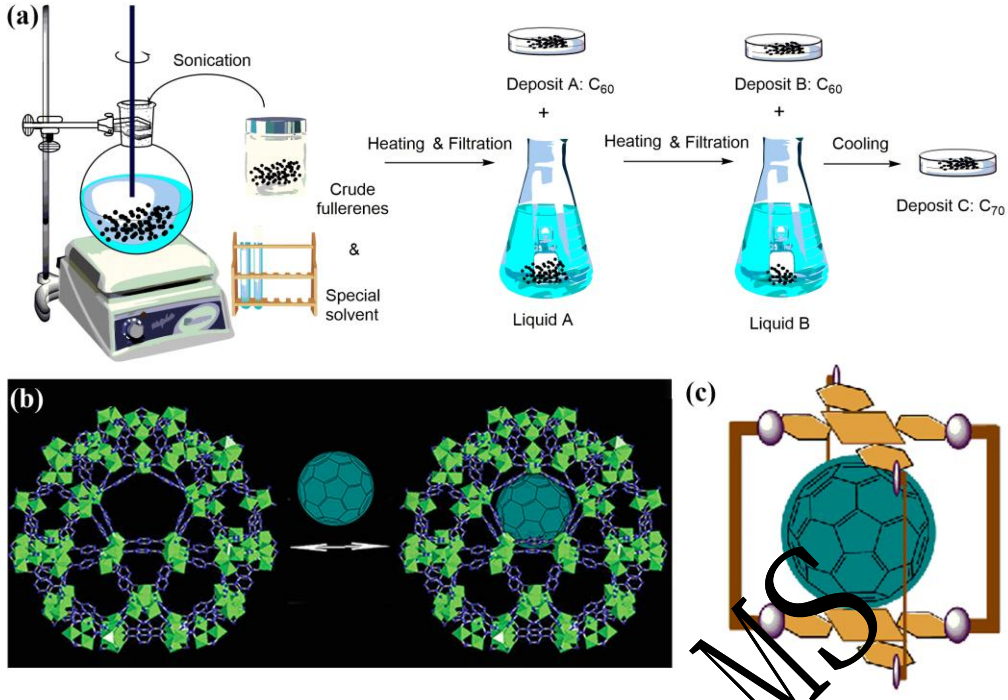

Fig. 2 Reported strategies of fullerene selective preparation: (a) fractional crystallization, (b) chromatographic method, (c) selective complexation with molecular receptor. Reprinted from Ref [64] with permission from Elsevier.

There are still some challenges in selective complexation method before applying in industrial preparation. On the one hand, it is not easy to determine the extent of reaction without visible phenomenon. On the other hand, the space of designed molecular receptors may be blocked by other materials with higher affinity than fullerenes, which also happens in chromatographic process. In a word, selective complexation, fractional crystallization, and chromatography are available, meanwhile greener technologies with recyclable process need to be further explored for selective preparation of fullerenes.

2.2 One-dimensional CNTs

CNTs, one-dimensional (1D) cylinder-shaped macromolecules, were found during the synthesis of fullerenes by arc discharge [93]. The diameter of CNT lies on the size of the semi-fullerene located at the end. Since they were found, CNTs have been the foci of numerous versatile fields due to their diameter- and helicity-dependent properties [94-96]. They are another one of the most representative examples of CNMs due to their excellent properties which are similar to fullerenes [97]. CNTs are classified into multi-walled carbon nanotubes (MWCNTs) and single-walled carbon nanotubes (SWCNTs), relying on the rolling layers of GR films.

Wide application of CNTs is reflected in the yield capacity which exceeds several thousand tons a year [98, 99]. Rapid innovations in the scalable production of CNTs have extended CNT research, like arc-discharge, laser ablation, and chemical vapor deposition (CVD) (Fig. 3) [98-100]. Among these methods, low-temperature plasma is a common used method owing to its multiple benefits, like widely distributed active species, improved catalyst activation, high-efficiency and sustainability in energy [101]. The low-temperature plasma contains positively charged ions, non-ionized atoms and free electrons which causes dissociation, ionization and excitation. Furthermore, this method can occur on the surface of materials without changing their main properties [101]. Laser ablation method is similar to low-temperature plasma. The advantage of laser ablation is to form high-purity

CNTs with defined chirality structure. But it is expensive and difficult for laser ablation to scale up in CNT selective preparation [100]. CVD method is mainly used for large-scale production of CNTs. CNTs are formed by the decomposition of CNTs precursor over transition metal catalyst and deposition. However, the prepared CNTs by CVD method show poor qualities that contain impurities, which is not suitable for CNT selective preparation [102].

For greener preparation of CNTs, cost-effective and eco-friendly approaches were reported to produce high quality MWCNTs. A recent preparation process used polymer waste like high-density polyethylene (HDPE) as the carbon source [103]. The conversion from polymer waste to MWCNTs happens in a closed environment via thermal dissociation with autogenic pressure and chemical catalysts. The first step is to add used HDPE which contains 20 wt% $C_4H_6CoO_4$ and cobalt acetate (CoAc) catalyst into a 5 cc autoclave. In the autoclave, the state and structure of HDPE change with the increase of reaction temperature in nitrogen atmosphere. Polymer waste begins to decompose at about 573 K and the outcomes containing water vapor, CO_2, and molecules with several carbon atoms can be recorded by Mass measurement. When temperature reaches above 873 K, the products include hydrogen, water vapor, and hydrocarbons. As the temperature up to 973 K, all the bonds of C-H and C-C start to get break, and the products consist of hydrocarbons and solid carbon coupled with hydrogen gas (Fig. 3d). This controlled dissociation of polymer waste is a reproducible technology for MWCNTs production, providing an opportunity for sustainable development and achieving a significant addition in industrial value.

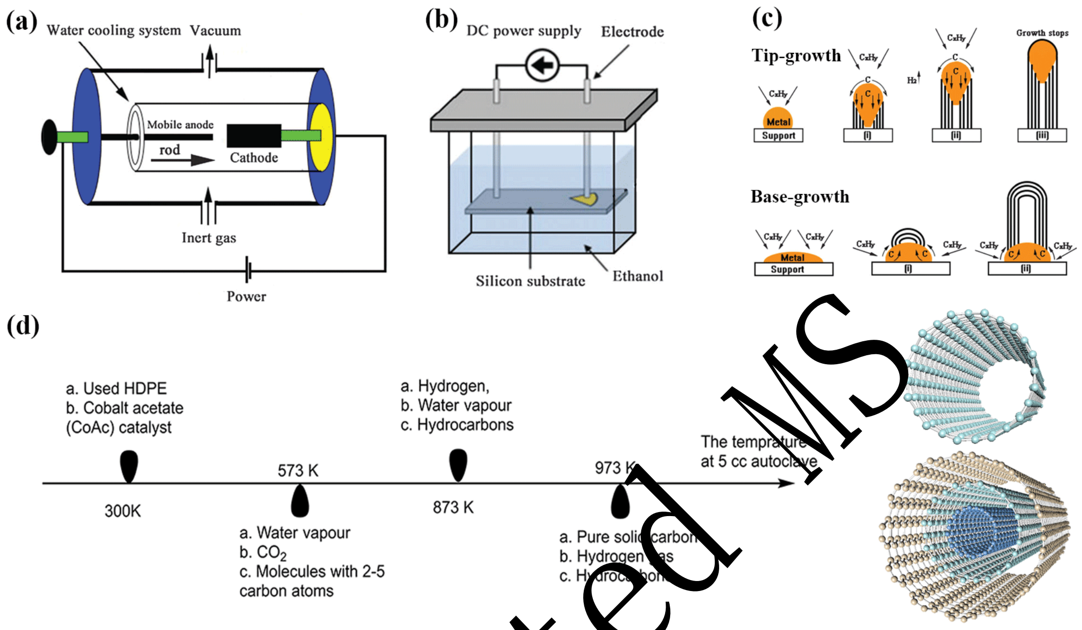

Fig. 3 Selective preparation of CNTs: (a, b) arc discharge technique, (c) CVD, (d) thermal dissociation of high-density polyethylene (HDPE). Reprinted from Ref [100] with permission from The Royal Society of Chemistry.

2.3 Two-dimensional GR

GR, the thinnest known material, is a two-dimensional (2D) carbon-based nanomaterial consisting of sp^2 bonded carbon atoms [104]. Since Geim and Novoselov seminal report on monolayer GR electronic properties [105], studies on its special properties, synthesis and various application have escalated sharply. Owing to the unique extended honeycomb network, GR can be used as the basic building block for other members of CNMs like 0D fullerene and 1D CNT [106]. GR reveals zero effective mass, giant intrinsic mobility in charge carriers, record thermal conductivity and stiffness [107-109]. And the electrons in GR show a linear dispersion and behave like massless relativistic particles, showing optical transparency, ambipolar electric field effect, transport via relativistic Dirac fermions and the quantum Hall effect [110, 111]. Because of these unique properties, GR shows the potential to promote the transfer of charge carriers along its planar surface. Hence, GR has been regarded as a promising candidate to be applied in photocatalysis [112-114].

Usually, there are four main methods for mass manufacture of pristine GR: (i) Extended GR. It contains CVD growth on epitaxial bound to the surface of metal substrates. May et.al. [115] first explained about extended GR without rationalizing the low-energy electron diffraction modes of a graphite monolayer.

(ii) Micromechanical exfoliation. Several studies elaborated on micromechanical exfoliation and outlined the great value for GR, inspiring continuous exploration in their potential science and applications [116-118].

(iii) Exfoliation of graphite. This typical method is making graphite powders exposed in organic solvents with high intensity ultrasound [119].

(iv) Other methods, such as bottom-up synthesis [120], growth on substrates [121], and arc discharge [122]. Issues of control in GR layers and minimization in folds have been solved via these methods.

Now the effort is made to achieve large-scale preparation of GR sheets with ideal thickness, because their unique properties are almost only bound up with individual sheet [123]. However, GR sheets show the tendency to agglomerate irreversibly and even restack to form graphite in the presence of strong van der Waals forces and π-π stacking. Compared with other methods, chemical reduction process was more suitable for high-quality GR sheet preparation. Chua et.al. [124] summarized the state-of-the-art in GR preparation via reduction process, including more than fifty types of reducing agent. For mass manufacture, it is encouraged to prepare GR from graphite crystals via reduction of graphene oxide (GO) [125-127]. The reduction process is shown in Fig. 4a. Graphite crystal possesses strong van der Waals forces between GR sheets (Fig. 4b). If using graphite crystal as the initial material, the powerful van der Waals forces are required to be broken at first. Graphite oxide is the oxidized form of graphite with oxygen functionalities mainly containing carbonyl, carboxyl, epoxide and hydroxyl. These oxygen functionalities enlarge the interlayer spacing which can weaken the forces between GR sheets for easier exfoliation. GO (Fig. 4c) is an intermediate, which can be gained from graphite oxide via ultrasonication or mechanical stirring. GO mainly exists in the state of mono-, bi- or few-layer sheets. Lastly, GR (Fig. 4d) with defects can be obtained from GO reduction through thermal treatment, electrochemical technology or chemical reduction [126-128]. The reduction of oxygen functionalities on GO follows the mechanism exhibited in Fig. 5. The reduction of epoxide begins from a ring opening by reducing agents (e.g. iodides and hydrazine) and then elimination from the benzene ring (Fig. 5a). The first step of carbonyl group reduction is to form hydroxyl groups, and next is dehydration which affords olefins (Fig. 5b). The reduction of carboxyl starts from the protonation at α-position of C=C bond combined with C=O bond, and then decarboxylation to regenerate C=C bond (Fig. 5c) [129].

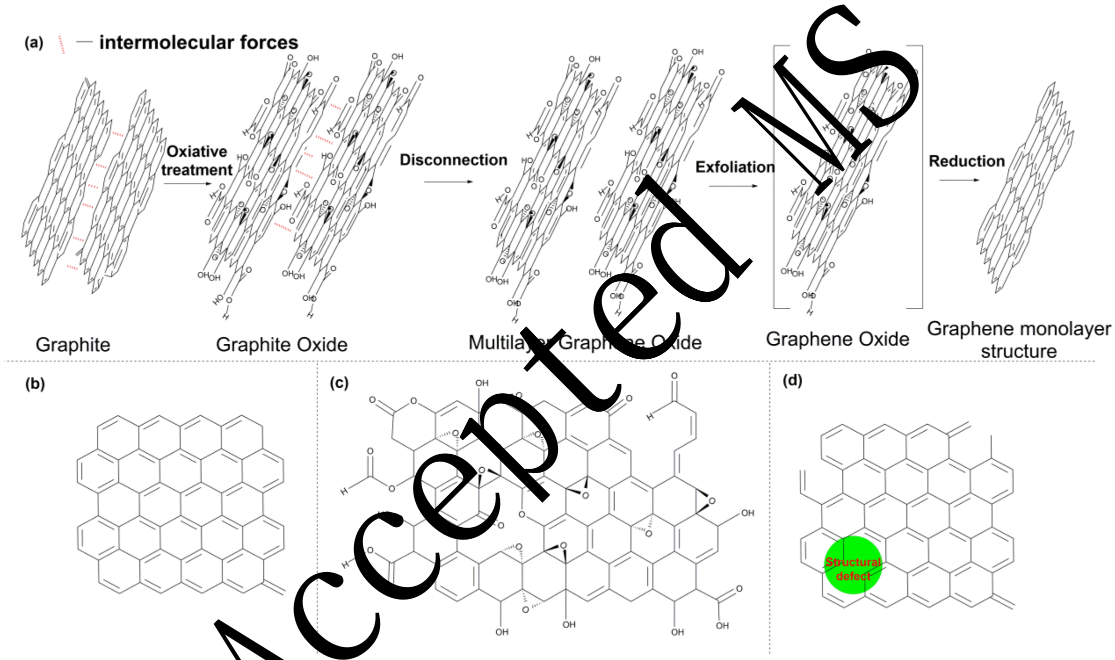

Fig. 4 (a) The process from graphite to GR; (b) Pristine mono-layer sheet of graphite; (c) Mono-layer sheet of graphite oxide or GO; (d) Synthesized mono GR from reduction of GO.

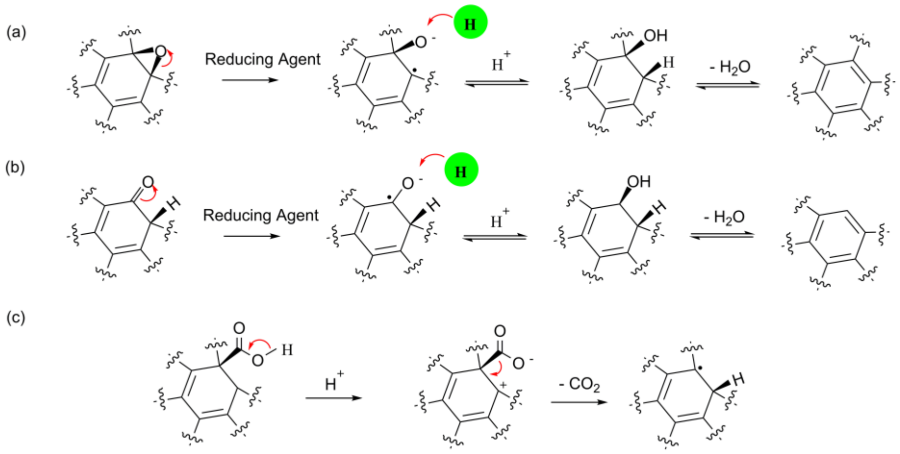

Fig. 5 (a) Reduction mechanism of epoxide on GR; (b) Reduction mechanism of carbonyl on GO; (c) Reduction mechanism of carboxyl on GO.

2.4 Three-dimensional CNMs-based networks

With the development of 0D fullerenes, 1D CNTs and 2D GR, macroscopic three-dimensional (3D) superlattices networks based on CNMs has received a huge amount of attention [130]. CNMs, constructed by sp^2 hybridized carbon atoms, can be used as building blocks for 3D networks fabrication (Fig. 6) [131]. Hexagonal carbon rings were not employed in the covalently interconnection with CNMs at multi terminal nodes. The mechanical properties of 3D networks for axial compression was unprecedented because of the covalent interconnections. On the other hand, 3D superlattices revealed porosity properties, minimized agglomeration and re-stacking, remarkable surface and electrical properties. These significant properties endows the 3D networks with the potential to be used for the fabrication of novel promising materials applied in catalytic process, environmental pollution treatment (e.g. adsorption and filtration), and molecular storage. Previously, Nardecchia, Chabot, and Dasgupta et.al. [130-132] elaborated on the synthesis of 3D networks, containing GR-, GO- CNT-based structures, and GR/CNT hybrid structures. Therefore, this section just make a brief summarization and focus on the potential properties that can be utilized in addressing environmental pollution and energy crisis.

There are many methods for the synthesis of 3D CNMs-based networks, such as hydro-/solvo-thermal process, template directed approaches, reduction, self-assembly, CVD, free standing direct dry and so on [133-136]. 3D networks fabricated via template directed approaches showed superhydrophobicity, high organic solvent and oil capacity. 3D networks constructed through free standing direct dry possessed scalable size, high strength and rigidity. Self-assembled 3D networks revealed benign elongation, high adsorption with reversible characteristic, and rapid compression recovery. All the synthesized 3D CNMs-based networks were found to behave high conductivity and chemical stability, which showed the potential application in the fabrication of novel CNMs-based materials for advanced photocatalytic application in environmental pollutant treatment and hydrogen production.

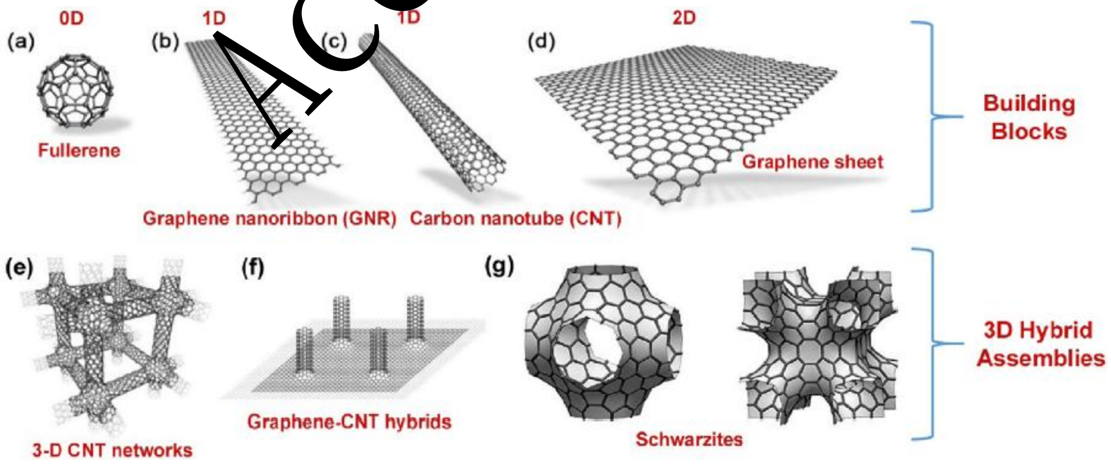

Fig. 6 0D, 1D, and 2D CNMs used as building blocks for 3D networks fabrication. Reprinted from ref [131] with permission from Elsevier.

3. Advanced photocatalytic application of CNMs

CNMs, revealing remarkable conductivity, thermostability, adsorptivity and controllability with delocalized conjugated structures, have a great impact on electron transfer process [40, 126, 137]. And specially, the surface properties of CNMs can be adjusted through chemical modification, which provides many opportunities for functionalized composites [121, 138]. To date, CNMs have gained extensive attention in photocatalysis field. Generally, the enhanced photocatalytic performance caused by the introduction of CNMs was ascribed to two aspects: (i) higher absorption capability in light due to their black body properties, (ii) longer life span of electron-hole pairs because CNMs play as an electron reservoir to trap photogenerated electrons [70, 73, 139, 140]. Since CNMs have similar structure and electronic properties in common, there is a question that whether all the CNMs play similar roles in the improvement of photocatalytic activity.

3.1 Environmental pollutant treatment

In photocatalytic process, CB electrons (e^-) and valence band holes (VB h^+) are produced when CNMs-modified photocatalysts are irradiated with light [141]. Electrons can directly reduce environmental pollutants like bromate, or be transferred to electron acceptors (i.e. CNMs) to react with molecular oxygen to produce superoxide radical species for oxidation of organic pollutants [142, 143]. Holes with strong oxidizing property plays a direct role in photocatalytic oxidation process, or react with adsorbed hydroxyl ions to produce hydroxyl radicals [144]. The photocatalytic application of CNMs in degradation of organic dyes was shown in Table 1, and the application in treatment of colorless organic and inorganic pollutants was shown in Table 2.

3.1.1 Degradation of organic dyes

A large scale of organic dyes from dye manufacturing and textile industries have been released into water environment over the past decades. Many of these dyes, such as Rhodamine B (RhB), methylene blue (MB) and methyl orange (MO), are toxic and carcinogenic. RhB and MB are dissolved in cationic, while MO are dissolved in anionic. Different from other organics and inorganics, colorful dyes can be photodegraded via three possible reactions: photosensitization, photolysis, and photocatalysis [145]. In photosensitization process, light irradiation can stimulate the dye to produce photo-electrons to transfer to conduction band of photocatalyst, then react with oxygen to form $\bullet O_2^-$. In photolysis process, electrons induced from the dye react with oxygen to form singlet oxygen atom for the oxidative degradation of dye.

CNMs-modified photocatalysts revealed high photocatalytic activity on the degradation of organic dyes owing to the introduction of π-system or the formation of heterojunctions [146]. For example, 0D C_{60} modified $Bi_2TiO_4F_2$ hierarchical microspheres showed strong photocatalytic performance for RhB degradation [70], and 1D TiO_2@MWCNTs composite show high degradation performance on MB and RhB [147]. Compared with 0D and 1D CNMs, 2D CNMs (e.g. GR, GO, and reduced

GO) reveal better interaction with photocatalysts. Reduced GO (rGO)/bismuth tungstate (BWO) composite, prepared in the presence of GO, showed high photocatalytic performance on the degradation of RhB (Fig. 7) [148]. The presence of GO promoted the interaction with the cations and provided reactive sites for the growth of nanoparticles. Introduction of rGO led to the negative shift of the Fermi level and the decrease in CB potential of BWO, promoting the migration of photoinduced electrons [149]. And owing to the excellent charge-carrier mobility of GR, separation of photogenerated electron-hole pairs on BWO was improved. GO reduction level has a positive impact on the photocatalytic performance of rGO/BWO.

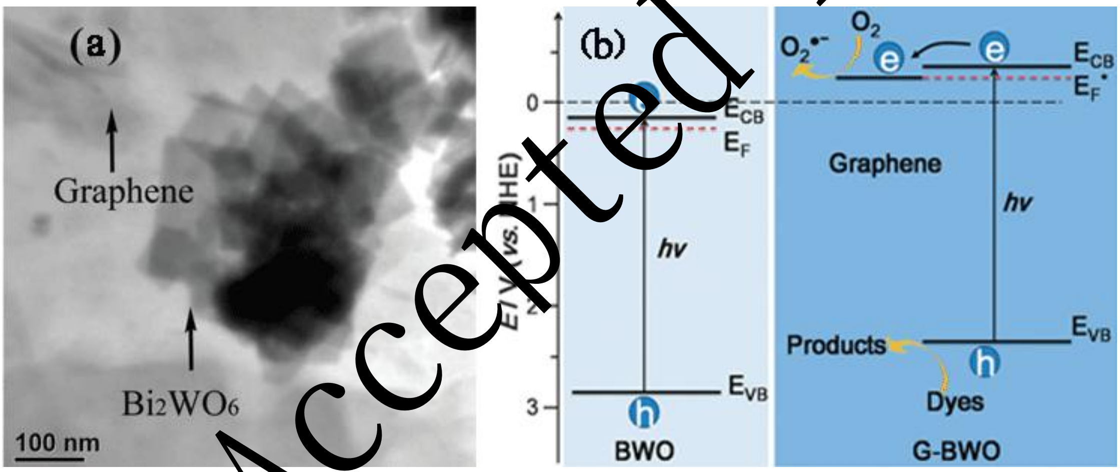

Fig. 7 (a) TEM image of GR/BWO composite; (b) Photocatalytic mechanism of organics degradation over GR/BWO composite. Reprinted from ref [148] with permission from The Royal Society of Chemistry.

Table 1 Photocatalytic application of CNMs in dye degradation.

Composites	Preparation process	Dye	Efficiency	Ref
C_{60}/g-C_3N_4	(i) ball-mill C_{60} and dicyandiamide; (ii) heat at 550 ℃ for 4 h.	MB	99.9%	[69]
C_{60}/$Bi_2TiO_4F_2$	(i) dissolve TiF4 into tert-butyl alchol; (ii) add Bi(NO_3)-ethylene glycol solution; (iii) add C60-toluenen solution, and heat at 160 ℃ for 24 h.	RhB	93.0%	[70]
GR-CQDs/g-C_3N_4	(i) CQDs was loaded on g-C_3N_4 through hydrothermal process; (ii) GO was reduced and combined with CQDs/g-C_3N_4 thorough a second hydrothermal process.	MO	91.1%	[146]
TiO_2@MWCNTs	(i) add MWCNTs into ethanol to make suspension; (ii) add $TiCl_4$ ethanol solution with sonication; (iii) heat at 150 ℃ for 3 h, and calcined at 600 ℃ for 5 h.	MB RhB	99.9% 99.9%	[147]
GR/BWO	(i) add GO to Bi(NO_3)$_3$·5H_2O solution; (ii) add Na_2WO_4·2H_2O, and adjust pH to about 7; (iii) heat at 180 ℃ for 16 h to obtain GO-BWO; (iv) mix GO-BWO with ethylene glycol, heat at 140 ℃ for 2 h.	RhB	99.9%	[148]

3.1.2 Oxidation of organic pollutants

Disposal and management of organic pollutants existing in air, water, and soil mediums is of great environmental concern [150]. CNMs are a nice choice to be applied in photocatalytic degradation of organic pollutants [126, 127]. For example, C_{60}-modified ZnAlTi-LDO showed high photocatalytic performance on the degradation of Bisphenol A (BPA) [151]. Besides, MWCNT-doped TiO_2 films were presented as efficient materials for photocatalytic degradation of PNP (Fig. 8) [152]. The electrical connection between MWCNTs and TiO_2 allows an easy transfer of photoinduced electrons from TiO_2 to conductive MWCNTs, leading to higher photocatalytic activity. The amount of MWCNTs introdcued to TiO_2 was limited under 4 wt%. Too high MWCNTs content would change the transparency of the film and isolate TiO_2 from touching light, then reduce the photocatalytic activity [152].

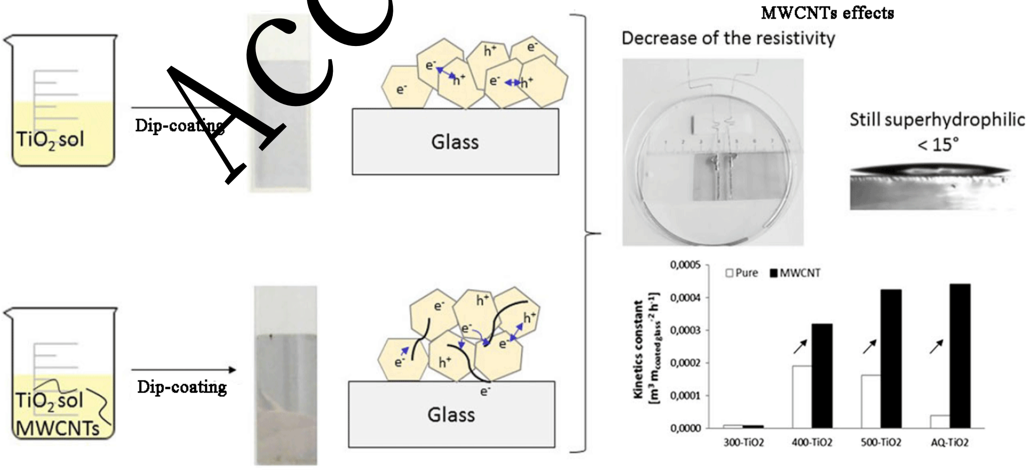

Fig. 8 Preparation of MWCNT-doped TiO_2 films and photocatalytic performance of as-prepared samples. Reprinted from ref [152] with permission from Springer**.**

Recently, we synthesized a 0D CQDs modified 2D BWO nanosheets hybrid material (CBW) for MO and BPA degradation [139]. CQDs are a new 0D member with size below 10 nm in the family of CNMs. Since the original report of CQDs in 2006 [153], they have attracted enormous attention because of their remarkable physical and chemical properties, like biocompatibility, robustness, stability, and chemical inertness [154, 155]. CQDs show unique both up- and down-PL, and that make CQDs-modified photocatalysts become near infrared light driven materials [156-158]. And ultrathin 2D BWO are excellent photocatalysts owing to their large specific surface area and special surface structure [159]. CBW composites with 0D/2D unique nanostructure possess four benefits: (i) well-structured accessible area between CQDs and m-BWO and the channels of bulk-to-surface for electrons transfer; (ii) the ability to utilize full spectrum of solar energy; (iii) improved adsorption capacity for pollutants (especially the hydrophobic pollutants) because of the CQDs sp^2 carbon clusters; (iv) enhanced interfacial charge transfer process owing to the efficient contact with pollutants caused by the ultra-small nanostructure (Fig. 9) [139].

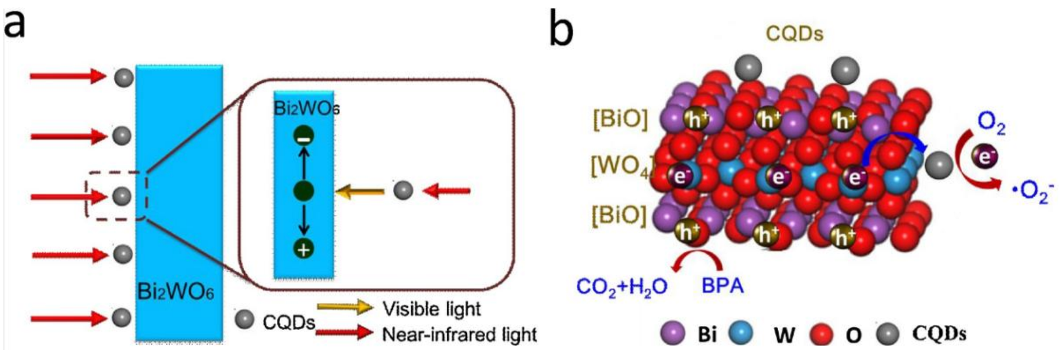

Fig. 9 (a) Schematic diagram for up converted PL of 0D CQDs modified 2D ultrathin BWO nanosheets heterojunctions; (b) proposed photocatalytic mechanism of CBW under full spectrum light irradiation. Reprinted from ref [139] with permission from Elsevier.

Many other CNMs have also been used in photocatalytic process for organic pollutant treatment. For example, kim et.al. [160] explored an improved method for the preparation of 1D carbon nanofiber (CNF)/titanate nanotube (TiNT) composite with a core-shell structure, and CNF-TiNT showed wonderful photocatalytic performance for the oxidation of gaseous acetaldehy. In addition, Zhao et.al. [161] recently reported a N-wrapping/bridging melamine-GR-TiO_2 capsule after H_2 treatment (H-TiO_2/MG-D) for efficient photocatalytic degradation of gaseous formaldehyde (HCHO). The introduction of GR improved the electrical conductivity of photocatalyst and the separation of charge carriers [161].

3.1.3 Treatment of inorganic pollutants

Inorganic pollutants caused a worldwide environmental concern due to their non-biodegradability, which will accumulate in biological bodies and lead to high-toxicity [131, 162]. Photocatalytic reduction over CNMs-modified materials has been proven to be an efficient method for inorganic pollutant treatment [112, 142]. For example, BWO/GR composites showed high photocatalytic performance on the oxidation of NO owing to the positive shift of the Fermi level cuased by GR [163], which is contrary to the negative shift caused by rGO [148].

GO and F co-doped TiO_2 (FGT) was presented to show high photocatalytic activity in the reduction of bromate (Fig. 10) [112]. Bromate, a common inorganic pollutant from the by-products of oxidation process for water purification, has been found to be strongly carcinogenic [164, 165]. The co-doping of GO and F enhanced the transportation of photogenerated e^- and the separation of charge carriers. In the photocatalytic process, a lower pH was beneficial for bromate reduction owing to the positive effect on bromate adsorption on FGT [112].

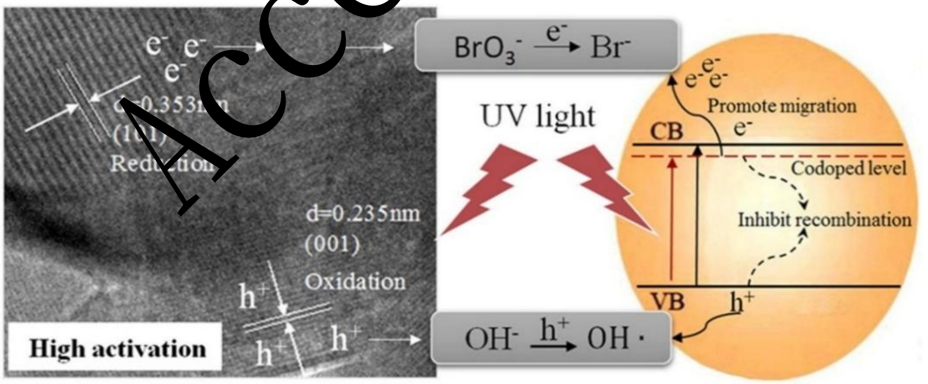

Fig. 10 Photocatalytic reduction of bromate by FGT: (a) cuboid morphologies with (001) and (101) facets; (b) spherical particles. Reprinted from ref [112] with permission from Elsevier.

Like NO and bromate, the existence of heavy metal ions in water and soil has been known to cause pollution problems. Photoreduction process is an efficient method to eliminate the toxicity of heavy metal ions by generating low toxic analogue ions [166]. For example, chromium (Cr), one of the most dangerous heavy metals, mainly consists of high-toxic Cr(VI) and low-toxic Cr(III) [167]. CNMs-modified composites show high photocatalytic performance on the removal of Cr(VI) [168-170].

Recently, a synthesized carbon dots (CDs)-TiO_2 nanosheets exhibited high photoactivity in the reduction of Cr(VI) (Fig. 11) [171]. The result of photocatalytic experiment over CDs-TiO_2 show that 99.2% Cr(VI) was reduced after 2 h irradiation [171]. CDs work as electron reservoir and donor, and they can play a favorable role in improving the photocatalytic performance by harvesting light and separating charge carriers.

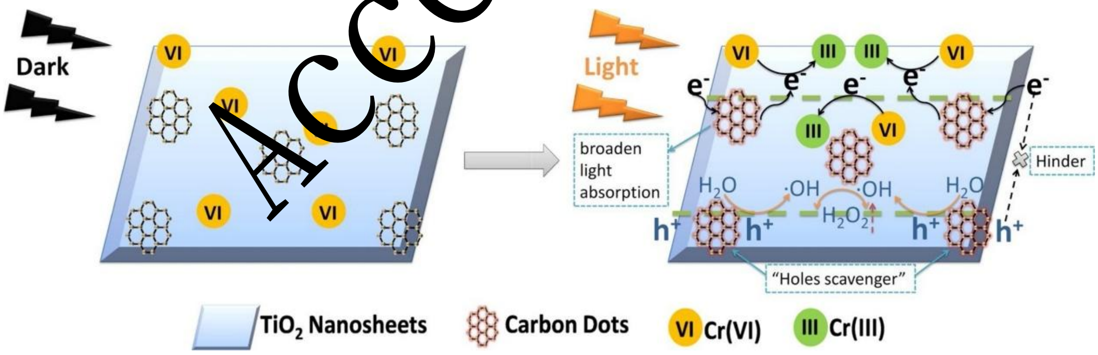

Fig. 11 Photoreduction process of Cr(VI) over CDs-TiO_2 nanosheets. Reprinted from ref [171] with permission from Elsevier.

Table 2 Photocatalytic application of CNMs in treatment of colorless organic pollutants and inorganics.

Composites	Preparation process	Pollutant Treatment	Efficiency	Ref
rGO/BWO	(i) electrostatic self-assembly of positively charged BWO and negatively charged GO sheets; (ii) hydrothermal treatment.	Oxidation of benzyl alcohol	93.0%	[149]
C_{60}-modified ZnAlTi-LDO	(i) combine ZnAlTi layered double hydroxide (ZnAlTi-LDH) with C_{60} via the urea method; (ii) calcine under vacuum atmosphere to obtain C_{60}-modified ZnAlTi layered double oxide (ZnAlTi-LDO).	Degradation of BPA	87.1%	[151]
MWCNT-doped TiO_2	(i) synthesize from two-step sol-gel routes: alcoholic and aqueous; (ii) deposited by dip-coating on glass.	Degradation of PNP	57%	[152]
CBW	(i) add $Na_2WO_4 \cdot 2H_2O$, $Bi(NO_3)_3 \cdot 5H_2O$, and cetyltrimethylammonium bromide into deionized water; (ii) add CQDs and stirring for 1 h; (iii) heat at 120 ℃ for 24 h.	Degradation of BPA	99.5%	[139]
CNF-TiNT	(i) mix nanosized TiO_2 and PAN to obtain TiO_2/PAN; (ii) carbonization to obtain TiO_x/CNFs; (iii) add TiO_x/CNFs to NaOH solution, heat at 150 ℃ for 24 h.	Oxidation of gaseous acetaldehy	95.4%	[160]
H-TiO_2/MG-D	(i) sonication: melamine and GO aqueous solution;	Degradation of	92.0%	[161]

	(ii) TiO_2/MG synthesis: add the mixture of tetrabutyl titanate and absolute ethanol to above solution, heat at 180℃ for 10 h; (iii) TiO_2/MG-D synthesis: mixed TiO_2/MG, hexamethyl tetramine, and dopamine hydrochloride solution, heat at 90℃ for 3 h, followed by H_2 treatment.	gaseous HCHO		
BWO/GR	(i) synthesize BWO through a hydrothermal method; (ii) mix GR and BWO, stir for 24 h.	Oxidation of NO	59.0%	[163]
FGT	(i) introduce GO, TiO2 and hydrofluoric acid to ethyl alcohol; (ii) heat at 180 ℃ for 24 h.	Reduction of bromate	99.9%	[112]
Ag@$BiVO_4$@rGO	(i) $BiVO_4$ were synthesized by maintaining the mixture of $Bi(NO_3)_3 \cdot H_2O$, NH_4VO_3 and $CO(NH_2)_2$ at 80 ℃ for 24 h; (ii) $BiVO_4$@rGO was synthesized by rGO chemical deposition; (iii) Ag@$BiVO_4$@rGO was gained by $AgNO_3$ photoreduction.	Reduction of bromate	99.1%	[165]
CuS/rGO	(i) mix GO and $CuSO_4 \cdot 5H_2O$ into deionized water with stir; (ii) treat at 160 ℃ with microwave irradiation.	Reduction of Cr(VI)	95.0%	[168]
CDs-TiO_2	(i) citric acid monohydrate were used as carbon source, $NH_3 \cdot H_2O$ were used as base, then mixed with TiO_2; (ii) heat at 160 ℃ for 4 h.	Reduction of Cr(VI)	99.2%	[171]

3.1.4 Photocatalytic disinfection

Bacteria exist almost everywhere. Several kinds of bacteria are harmful for human, such as *Escherichia coli* (*E. coli*), *staphylococcus aureus* (*S. aureus*), *Fusarium oxysporum* (*F. oxysporum*), and *pneumococcus aeruginosa* (*P. aeruginosa*). These harmful bacteria can enter human body via eating and breathing, and then cause diseases. Photocatalysis has been proven to be an efficient method for disinfection owing to the great oxidation ability [172-174]. Generally, photocatalytic disinfection contains two main sequential processes: (i) generation of reactive oxygen species (ROS) after light irradiation and (ii) the attack of ROS on bacterial cells. To fully understand the mechanism of photocatalytic disinfection, it is necessary to first identify the detailed effect of ROS (e.g. singlet oxygen, $\bullet O_2^-$, •OH, and H_2O_2) on the disinfection performance of photocatalysts.

Until today, many CNMs-modified photocatalysts have been synthesized and applied in disinfection [175-177]. CNMs in composite photocatalysts can boost the electron reduction of oxygen to generate more ROS. For example, rGO in TiO_2/rGO composite photocatalyst can boost the production of H_2O_2 [178]. Moreover, CNMs can react with photocatalysts to form chemical bonds to enhance the activity, such as the formed Ti-O-C and Ti-OH in MnO_x quantum dots decorated rGO/TiO_2 [179]. Recently, Zhang et.al. [175] presented a CDs and TiO_2 co-decorated rGO (CTR) ternary composite photocatalyst for *E. coli* inactivation (Fig. 12). The result showed that CTR slurry system reached 1.03 log inactivation of *E. coli* after 60 min of light irradiation. CDs play as both electron acceptor and donor and GR work as a scaffold, also enhancing the single electron transfer for O_2 reduction to form $•O_2^-$. Besides, Cruz-Ortiz et.al. [176] explored the mechanism of photocatalytic disinfection using TiO_2-GR composite photocatalysts under UV and visible irradiation. In this study, the generated ROS under light irradiation were investigated. It was found that H_2O_2 worked as a dominant ROS in the inactivation of *E. coli* under UV light, but singlet oxygen played a dominant role under visible light [176]. And chloride was presented to have an effect on the disinfection performance of photocatalysts. Chloride can react with ROS in photocatalytic process to form chlorine, which then consume H_2O_2 to form singlet oxygen [176]. In addition, our previous study found that humic acid might limit the physical contact between bacterial cells and photocatalysts [177].

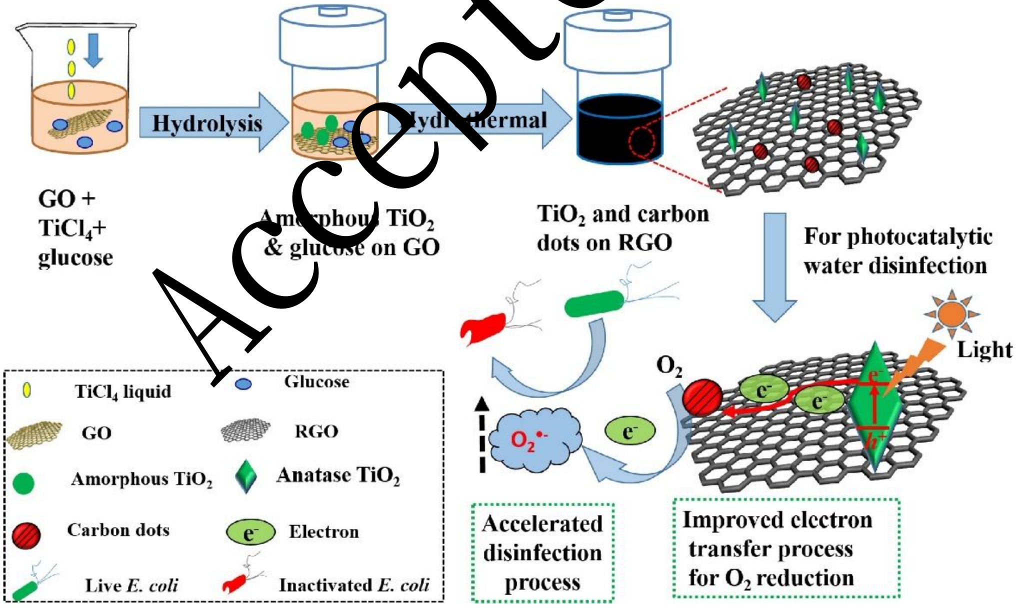

Fig. 12 Synthesis of CTR nanocomposite and application in photocatalytic disinfection. Reprinted from ref [175] with permission from Elsevier.

In conclusion, CNMs played three important roles in the enhanced photocatalytic disinfection. Firstly, CNMs worked as a scaffold to avoid the aggregation of photocatalysts in the CNMs-based composite photocatalysts. Secondly, conductive CNMs worked as an electron acceptor or donor to improve the separation of charge carriers and promote electron reduction of oxygen to form H_2O_2. Thirdly, chemical bonds formed between CNMs and photocatalysts can improve the performance in photocatalytic disinfection.

3.2 Hydrogen production

Photocatalytic water-splitting technology over CNMs-modified materials has shown great potential for hydrogen production owing to the low cost and high sustainability [180-182]. Water-splitting includes two half reactions: (i) hydrogen evolution reaction and (ii) oxygen evolution reaction. Photogenerated e^- are the main substances in hydrogen evolution reaction via reduction process, and CB level of CNMs-modified photocatalysts should be more negative than hydrogen production level. The efficiency of photocatalytic hydrogen production depends on the quantum conversion of the absorbed light to photogenerated e^- - h^+ pairs and the separation efficiency of charge carriers. The photocatalytic application of CNMs in hydrogen production was shown in Table 3.

For example, 3D $CoSe_2$-CNT microspheres was presented for hydrogen production, and it was prepared via combined spray pyrolysis and selenization process (Fig. 13) [56]. This $CoSe_2$-CNT composites showed remarkable catalytic activity with an overpotential of ~174 mV at 10 mA cm^{-2} and excellent durability in an acidic medium. The backbone of CNTs provided a porous way for the acidic liquid medium to go through the microspheres. Hence, the contact area of $CoSe_2$ active sites with the reaction medium was improved, which leading to the enhancement of the electrocatalytic activity for more efficient hydrogen evolution.

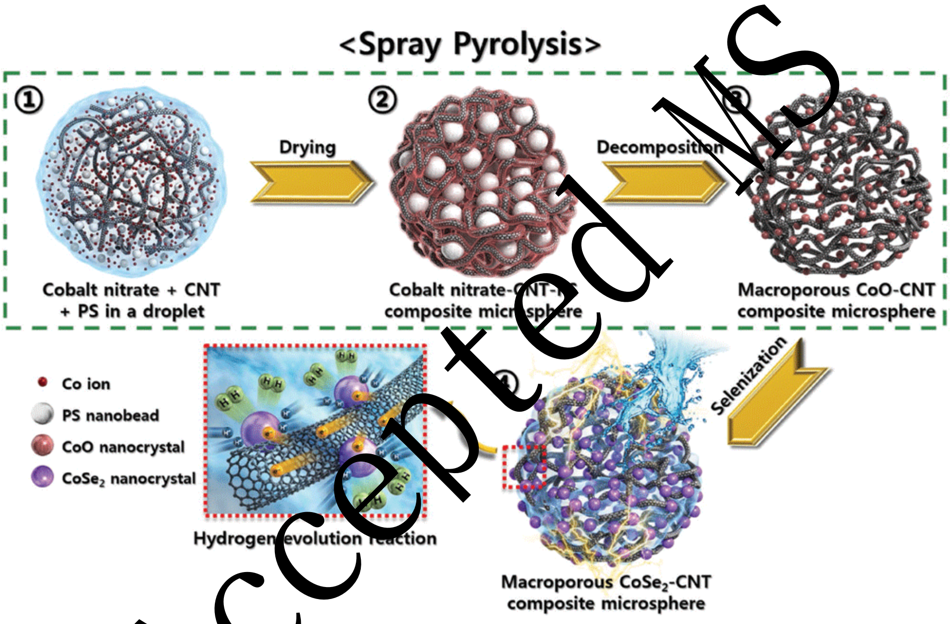

Fig. 13 Proposed mechanism of $CoSe_2$-CNT composite microspheres through spray pyrolysis process and one-step post treatment. Reprinted from ref [56] with permission from Wiley.

Additionally, 2D rGO with a suitable reduction degree was utilized to prepare rGO-BWO photocatalyst for hydrogen production [57]. CB of rGO, composed of antibonding π^* orbitals, is more negative than the standard redox potential of H_2O/H_2. Therefore, efficient H_2 production over rGO-BWO was contributed to the more negative reduction potential caused by the introduction of rGO. And in the process of H_2 generation, lactic acid was added as a sacrificial reagent into aqueous methanol solution to promote the photocatalytic performance. Moreover, photocatalytic process over rGO-BWO can also be used for O_2 generation with adding Fe^{3+} ions as electron acceptor. E_{VB} of rGO-BWO is more positive than the standard redox potential of O^{2-}/O_2, which ensures the conversion of H_2O to O_2. The higher O_2 production was ascribed to the strong chemical bonding between rGO and BWO, which promoted the electron collection, transportation and the separation of photoinduced charge carriers (Fig. 14). Very recently, Marcelo et.al. [183] explored the photo-proton effect of GR, and did an experiment of shining a light on GR decorated with Pt, which revealed high performance on hydrogen production. Liu et.al. [184] reported that an synthesized $MoS_2QDs@ZnIn_2S_4@RGO$ showed high photocatalytic performance on hydrogen production with simultaneous water purification.

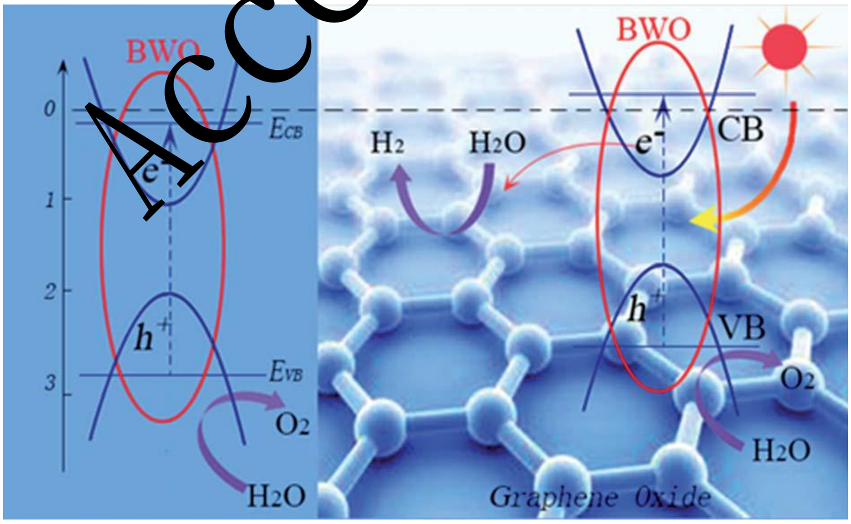

Fig. 14 Proposed mechanism of the photocatalytic activity of GR-BWO composite. Reprinted from ref [57] with permission from The Royal Society of Chemistry.

Emerging 0D CQDs has also been used to enhance the photocatalytic performance in hydrogen production [185-188]. For example, CQDs/MoS_2 (Fig. 15) prepared through hydrothermal process showed high reduction activity for hydrogen evolution under visible light irradiation [189]. CQDs modified on the surface of MoS_2 makes the electrocatalytic activity more efficient with an overpotential of ~0.125 V at 10 mA cm^{-2} and show good stability in sulphuric acid. The enhanced performance is ascribed to the high charge transfer efficiency caused by the introduction of CQDs, and the decrease of S^{4+} and the increase of disulfides S_2^{2-} and apical S^{2-} [185]. Disulfides S_2^{2-} and apical S^{2-} are the active sites for hydrogen evolution reduction after visible light irradiation [185]. The preparation of this CQDs/MoS_2 composite provides a potential alternative approach for the design of cost-efficient electrocatalysts with enhanced catalytic performance, instead of introducing other heteroatom doped carbons.

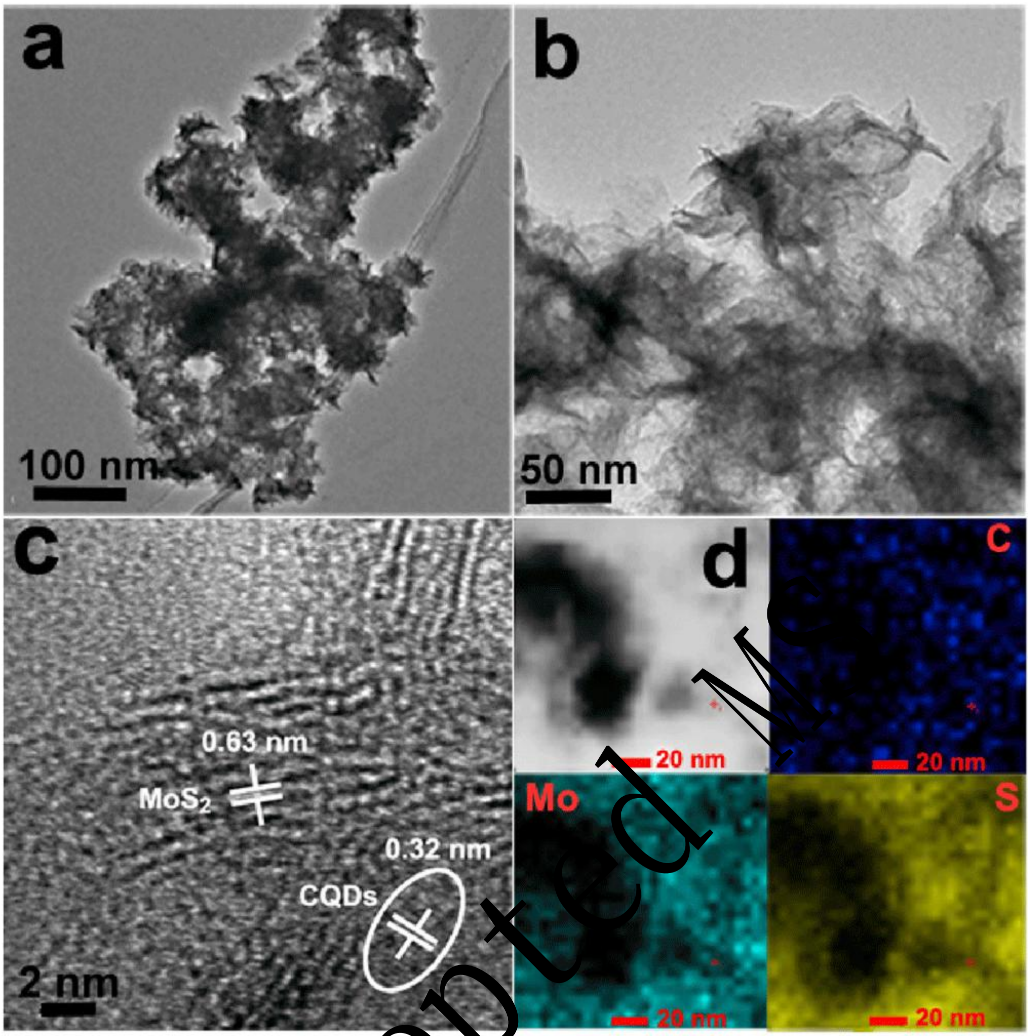

Fig. 15 Characterization of the CQDs/MoS_2 composite: (a) Low magnification TEM image; (b) High magnification TEM image; (c) High resolution of TEM image; (d) SEM image. Reprinted from ref [189] with permission from Elsevier.

Besides, CNMs-modified photocatalysts prepared with designed structure were reported to be efficient for hydrogen production, like hierarchical core-shell CNF@$ZnIn_2S_4$ (Fig. 16) [190]. $ZnIn_2S_4$, a metal sulfide, has been widely studied owing to the suitable band gap and visible-light driven photocatalytic functions. In CNF@$ZnIn_2S_4$, CNF acted as the electron acceptor that transported the photogenerated electrons in CB of $ZnIn_2S_4$ along the cylindrical nanostructure. The hierarchical core-shell configuration structure was beneficial for the formation of an intimate contact between CNF core and $ZnIn_2S_4$ sheets, which accelerated the interfacial charge transfer of $ZnIn_2S_4$. And to ensure the efficiency of charge transfer and the separation of photoexcited electron-hole pairs, sacrificial reagent was added to complement the electrons to combine with the holes in VB of $ZnIn_2S_4$. CNF content has an impact on the photocatalytic performance, and the optimum content is located at 15 wt % [190]. Low CNF content will lead to the formation of $ZnIn_2S_4$ microspheres separated from CNF, while high content will hinder the generation of photoinduced electrons and holes on $ZnIn_2S_4$.

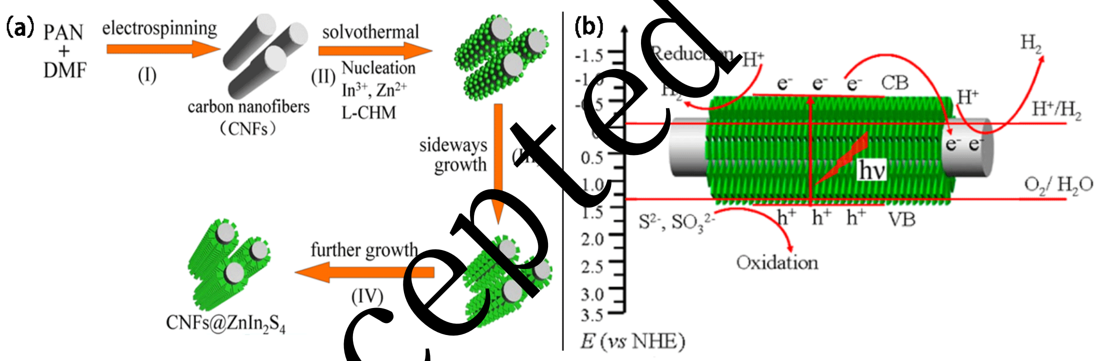

Fig. 16 (a) Formation process of the hierarchical core−shell $CNFs@ZnIn_2S_4$ composites; (b) proposed photocatalytic mechanism of hydrogen evolution over the hierarchical core shell CNFs@ZnIn2S4 composites. Reprinted from ref [190] with permission from American Chemical Society.

613 Table 3 Photocatalytic application of CNMs in hydrogen production.

Materials	Preparation process	Clean-energy	Ref
$CoSe_2$-CNT	(i) dry droplet formed by $Co(NO_3)_2$•$6H_2O$, CNTs and polystyrene nanobeads; (ii) decomposition, partial reduction, then selenization.	Hydrogen	[56]
TiO_2@MWCNTs	(i) mix MWCNTs ethanol solution and $TiCl_4$ ethanol solution; (ii) heat at 150 ℃ for 3 h, and calcine at 600 ℃ for 5 h.	Hydrogen	[147]
MWCNT-doped TiO_2	(i) synthesize from two-step sol-gel routes: alcoholic and aqueous; (ii) deposited by dip-coating on glass.	Hydrogen	[152]
GR-BWO	(i) dissolve $Bi(NO_3)_3 \cdot 5H_2O$ in 6.5% HNO_3 solution and then add GO; (ii) add $(NH_4)_{10}W_{12}O_{14}$ solution, adjust pH to 7 and stir at 50 ℃ for 2 h; (iii) 3 h of sonication with a high-intensity ultrasonic probe.	H_2 and O_2	[57]
MoS_2QDs@$ZnIn_2S_4$@RGO	(i) disperse GO in mixed dimethylformamide and ethylene glycol; (ii) add thioacetamide, $InCl_3 \cdot 4H_2O$ and $Zn(Ac)_2 \cdot 2H_2O$; (iii) heat at 180 ℃ for 12 h.	Hydrogen	[184]
CQDs/MoS_2	(i) synthesize CQDs via an electrochemical etching method; (ii) add CQDs to Na_2MoO_4 and L-cysteine mixed water solution; (iii) heat to 180 ℃ and maintain for 24 h.	H_2 and O_2	[189]
CNF@$ZnIn_2S_4$	(i) synthesize CNFs through an electrospinning apparatus; (ii) add glycerol, $In(NO_3)_3 \cdot 4.5H_2O$, $Zn(AC)_2 \cdot 6H_2O$, and L-cysteine hydrochloride monohydrate into CNFs ethanol solution; (iv) heat to 180 ℃ and maintain for 24 h.	Hydrogen	[190]

4. Limitation on wider application of CNMs

(i) The first limitation for wider industrial application of CNMs is the high cost of CNMs. Though the market price of CNMs are coming down all the time, it is still too expensive to be applied in industry (Table 4). To bring the price down, cheaper selective preparation for high quality CNMs are needed.

Table 4 Cost of several CNMs searched in CheapTubes.com (USA).

CNMs	Price (US/$ **g**$^{-1}$)
Fullerene C_{60} (99.9%)	225.00
Carbon fullerene C_{60}	35.00
SWCNT	>24.48
WMCNT	>0.6
GR	>2.5
rGO	400.00

(ii) For environmental pollutant treatment over CNMs-modified photocatalysts, many studies focused on single pollutant or confined to aqueous pollutants [131, 144, 147, 184]. However, there are numerous pollutants containing organics, heavy metal ions, inorganic salt ions and so on not only in water but also in air and soil environment. Therefore, to achieve efficient treatment on actual pollutions, further exploration on more efficient treatments for more complex water matrix and even whole environment matrix over CNMs-modified photocatalysts is required.

(iii) As for hydrogen production, there are also some challenges in practical operations. One main barrier for practical application is the difficulty in H_2 separation when H_2 and O_2 generated simultaneously from photocatalytic water splitting. Though the separation can be achieved by adding h^+ scavenger or O_2 trapping agent, the cost of the whole process would increase greatly [191]. Besides, today's reactors for hydrogen evolution are small and the yield fall far short of the needed quantity [192, 193]. Therefore, to develop a large-scale hydrogen production process is the other challenge.

5. Summary and Outlook

The importance of efficient pollutant treatment and hydrogen production is evident from the aggravation of environmental and energy crisis in "green" 21st century. Photocatalytic process over CNMs-modified photocatalysts is a highly-effective solution for the crisis owing to the remarkable morphological, mechanical, electrical and optical properties. Notably, CNMs show size- and structure-dependent properties in photocatalytic process. For example, C_{60} has been used in photocatalytic process more frequently than other higher fullerenes because of the smallest size, GR shows better performance in photocatalytic system comparing with 0D fullerene and 1D CNT owing to the 2D structure, and GR or CNT can contribute to constructing firm network structures with superior integrated performance due to the anisotropic structures. To date, many efforts have been made to take advantage of these unique size-and structure-dependent properties of CNMs. But researches on the optimization of structure-dependent properties are still in their infancy. A further exploration on the accurate relationship between structure and property need to be addressed. Besides, the selective preparation for desired structure and morphology in a sustainable and reversible way is a significant challenge for CNMs. Reducing costs, emissions and improving security of supply are supposed to be taken into account while locating the "sustainable energy trilemma" during the preparation process.

Therefore, in this review, we firstly summarize selective preparation of CNMs that has a great impact on their photocatalytic performance. Then we provide an updated outline of advanced photocatalytic application of CNMs in addressing both environmental pollution and hydrogen energy crisis. The difference in the role of various CNMs play in the enhancement of photocatalytic performance is also discussed. Lastly, we discuss the limitations of CNMs applied in photocatalysis or even wider fields.

CNMs-modified photocatalysts with different nanostructures ranging from 1D to 3D structures can been prepared through various methods, such as electrospinning, sol-gel process, deposition process, hydro- or solvo-thermal process, and sonochemical process. The optimization of operational parameters is significant for the preparation of CNMs-modified photocatalysts with revealing desirable charge carrier transport in photocatalytic process. Moreover, introduction of CNMs can enhance the photocatalytic performance owing to the enhanced absorption capability in light and efficient transport of photogenerated electrons. Commonly, CNMs act as absorbent, photostabilizer, co-catalyst, and photosensitizer. Besides, CNMs can play as can play as a template [194], surfactant or powerful plasmonic material [195], structure-directing and morphology-controlling agent [196], and even hole-extraction layers for the preparation of photocatalytic materials [197-199]. To maximize the effect of CNMs in improving the photocatalytic performance, all these functions are supposed to be studied at length, and other possible roles of CNMs playing in the composite photocatalysts are needed to be further explored. On the other hand, the exploration and optimization of synthesis process for large-scale high-quality CNMs-modified photocatalysts should proceed simultaneously. And greater efforts ought to be made in the combination of theoretical calculation and experimental evidence to investigate unclear mechanism for enhanced photoactivity of CNMs-modified materials. These mentioned aspects are critical factors for improving the photoactivity of CNMs-modified composites. We hope this review can promote the more objective understanding on the analogy, and strengthen the efforts towards the advanced photocatalytic application of these CNMs (including fullerenes, CQDs, CNFs, CNTs, and GR) in energy and environmental field.

Acknowledgements

This study was financially supported by the Program for the National Natural Science Foundation of China (51579098, 51779090, 51709101, 51278176, 51408206, 51521006, 81773333), Science and Technology Plan Project of Hunan Province (2017SK2243, 2016RS3026), the National Program for Support of Top-Notch Young Professionals of China (2014), the Program for New Century Excellent Talents in University (NCET-13-0186), the Program for Changjiang Scholars and Innovative Research Team in University (IRT-13R17), and the Fundamental Research Funds for the Central Universities (531107050978, 531107051080).

References

[1] B. Obama, The irreversible momentum of clean energy, Science, 355 (2017) 126-129.

[2] M. Cheng, G. Zeng, D. Huang, C. Yang, C. Lai, C. Zhang, Y. Liu, Tween 80 surfactant-enhanced bioremediation: toward a solution to the soil contamination by hydrophobic organic compounds, Crit. Rev. Biotechnol., 38 (2018) 17-30.

[3] L. Qin, G. Zeng, C. Lai, D. Huang, C. Zhang, P. Xu, T. Hu, X. Liu, M. Cheng, Y. Liu, L. Hu, Y. Zhou, A visual application of gold nanoparticles: Simple, reliable and sensitive detection of kanamycin based on hydrogen-bonding recognition, Sens. Actuators, B, 243 (2017) 946-954.

[4] D.L. Huang, C.J. Hu, G.M. Zeng, M. Cheng, P.A. Xu, X.M. Gong, R.Z. Wang, W.J. Xue, Combination of Fenton processes and biotreatment for wastewater treatment and soil remediation, Sci. Total Environ., 574 (2017) 1599-1610.

[5] M. Cheng, G. Zeng, D. Huang, C. Lai, P. Xu, C. Zhang, Y. Liu, Hydroxyl radicals based advanced oxidation processes (AOPs) for remediation of soils contaminated with organic compounds: A review, Chem. Eng. J., 284 (2016) 582-598.

[6] M. Cheng, G. Zeng, D. Huang, C. Lai, P. Xu, C. Zhang, Y. Liu, J. Wan, X. Gong, Y. Zhu, Degradation of atrazine by a novel Fenton-like process and assessment the influence on the treated soil, J. Hazard. Mater., 312 (2016) 184-191.

[7] B. Pan, Y. Zhou, W. Su, X. Wang, Self-assembly synthesis of $LaPO_4$ hierarchical hollow spheres with enhanced photocatalytic CO_2-reduction performance, Nano Res., 10 (2017) 534-545.

[8] J. Di, C. Yan, A.D. Handoko, Z.W. Seh, H. Li, Z. Liu, Ultrathin two-dimensional materials for photo- and electrocatalytic hydrogen evolution, Mater. Today, (2018).

[9] Y.-K. Peng, S.C.E. Tsang, Facet-dependent photocatalysis of nanosize semiconductive metal oxides and progress of their characterization, Nano Today, 18 (2018) 15-34.

[10] M. Han, S. Zhu, S. Lu, Y. Song, T. Feng, S. Tao, J. Liu, B. Yang, Recent progress on the photocatalysis of carbon dots: Classification, mechanism and applications, Nano Today, 19 (2018) 201-218.

[11] M. Zheng, J. Shi, T. Yuan, X. Wang, Metal‐Free Dehydrogenation of N‐Heterocycles by Ternary

h‑BCN Nanosheets with Visible Light, Angew. Chem. Int. Ed., 57 (2018) 5487-5491.

[12] L. Li, C. Cui, W. Su, Y. Wang, R. Wang, Hollow click-based porous organic polymers for heterogenization of $[Ru(bpy)_3]^{2+}$ through electrostatic interactions, Nano Res., 9 (2016) 779-786.

[13] A. Fujishima, K. Honda, Electrochemical photolysis of water at a semiconductor electrode, Nature, 238 (1972) 37.

[14] L. Wang, N. Xu, X. Pan, Y. He, X. Wang, W. Su, Cobalt lactate complex as a hole cocatalyst for significantly enhanced photocatalytic H_2 production activity over CdS nanorods, Catal. Sci. Technol., 8 (2018) 1599-1605.

[15] J.R. Ran, G.P. Gao, F.T. Li, T.Y. Ma, A.J. Du, S.Z. Qiao, Ti_3C_2 MXene co-catalyst on metal sulfide photo-absorbers for enhanced visible-light photocatalytic hydrogen production, Nat. Commun., 8 (2017).

[16] L. Li, W. Fang, P. Zhang, J. Bi, Y. He, J. Wang, W. Su, Sulfur-doped covalent triazine-based frameworks for enhanced photocatalytic hydrogen evolution from water under visible light, J. Mater. Chem. A, 4 (2016) 12402-12406.

[17] B. Pan, Y. Zhou, W. Su, X. Wang, Enhanced photocatalytic CO_2 conversion over $LaPO_4$ by introduction of $CoCl_2$ as a hole mediator, RSC Adv., 6 (2016) 34744-34747.

[18] A. Li, X. Chang, Z. Huang, C. Li, Y. Wei, L. Zhang, T. Wang, J. Gong, Thin heterojunctions and spatially separated cocatalysts to simultaneously reduce bulk and surface recombination in photocatalysts, Angew. Chem. Int. Ed., 55 (2016) 13734-13738.

[19] D.T. You, B. Pan, F. Jiang, Y.G. Zhou, W.Y. Su, CdS nanoparticles/CeO_2 nanorods composite with high-efficiency visible-light-driven photocatalytic activity, Appl. Surf. Sci., 363 (2016) 154-160.

[20] B. Pan, S. Luo, W. Su, X. Wang, Photocatalytic CO_2 reduction with H_2O over $LaPO_4$ nanorods deposited with Pt cocatalyst, Appl. Catal. B: Environ., 168-169 (2015) 458-464.

[21] S. Bai, J. Jiang, Q. Zhang, Y. Xiong, Steering charge kinetics in photocatalysis: intersection of materials syntheses, characterization techniques and theoretical simulations, Chem. Soc. Rev., 44 (2015) 2893-2939.

[22] J. Qian, Z. Peng, M. Peng, H. Li, M. Wang, H. Li, X. Fu, Carbon fibers@semiconductors nanostructures core-shell composites: Facile strategy for highly efficient solar-driven photocatalysts, J. Catal., 353 (2017) 325-334.

[23] I. Velo-Gala, J.J. López-Peñalver, M. Sánchez-Polo, J. Rivera-Utrilla, Role of activated carbon surface chemistry in its photocatalytic activity and the generation of oxidant radicals under UV or solar radiation, Appl. Catal., B, 207 (2017) 412-423.

[24] M. Chen, S. Zhou, G. Zeng, C. Zhang, P. Xu, Putting carbon nanomaterials on the carbon cycle map, Nano Today, (2018).

[25] J. Yan, C.E. Ren, K. Maleski, C.B. Hatter, B. Anasori, P. Urbankowski, A. Sarycheva, Y. Gogotsi, Flexible MXene/graphene films for ultrafast supercapacitors with outstanding volumetric capacitance, Adv. Funct. Mater., 27 (2017).

[26] Z.-L. Xu, J.-K. Kim, K. Kang, Carbon nanomaterials for advanced lithium sulfur batteries, Nano Today, 19 (2018) 84-107.

[27] E.S. Cho, A.M. Ruminski, S. Aloni, Y.-S. Liu, J. Guo, J.J. Urban, Graphene oxide/metal nanocrystal multilaminates as the atomic limit for safe and selective hydrogen storage, Nat. Commun., 7 (2016).

[28] M. Rudolf, S.V. Kirner, D.M. Guldi, A multicomponent molecular approach to artificial photosynthesis - the role of fullerenes and endohedral metallofullerenes, Chem. Soc. Rev., 45 (2016)

612-630.

[29] J. Bartelmess, S.J. Quinn, S. Giordani, Carbon nanomaterials: multi-functional agents for biomedical fluorescence and Raman imaging, Chem. Soc. Rev., 44 (2015) 4672-4698.

[30] X.J. Hu, J.S. Wang, Y.G. Liu, X. Li, G.M. Zeng, Z.L. Bao, X.X. Zeng, A.W. Chen, F. Long, Adsorption of chromium (VI) by ethylenediamine-modified cross-linked magnetic chitosan resin: Isotherms, kinetics and thermodynamics, J. Hazard. Mater., 185 (2010) 306-314.

[31] C. Zhang, C. Lai, G. Zeng, D. Huang, L. Tang, C. Yang, Y. Zhou, L. Qin, M. Cheng, Nanoporous Au-based chronocoulometric aptasensor for amplified detection of Pb^{2+} using DNAzyme modified with Au nanoparticles, Biosens. Bioelectron., 81 (2016) 61-67.

[32] W.-W. Tang, G.-M. Zeng, J.-L. Gong, J. Liang, P. Xu, C. Zhang, B.-B. Huang, Impact of humic/fulvic acid on the removal of heavy metals from aqueous solutions using nanomaterials: a review, Sci. Total Environ., 468 (2014) 1014-1027.

[33] P. Xu, G.M. Zeng, D.L. Huang, C. Lai, M.H. Zhao, Z. Wei, N.J. Li, C. Huang, G.X. Xie, Adsorption of Pb(II) by iron oxide nanoparticles immobilized Phanerochaete chrysosporium: Equilibrium, kinetic, thermodynamic and mechanisms analysis, Chem. Eng. J., 203 (2012) 423-431.

[34] J. Liang, Z. Yang, L. Tang, G. Zeng, M. Yu, X. Li, H. Wu, Y. Qian, X. Li, Y. Luo, Changes in heavy metal mobility and availability from contaminated wetland soil remediated with combined biochar-compost, Chemosphere, 181 (2017) 281-288.

[35] J. Wan, G. Zeng, D. Huang, L. Hu, P. Xu, C. Huang, R. Deng, W. Xue, C. Lai, C. Zhou, K. Zheng, X. Ren, X. Gong, Rhamnolipid stabilized nano-chlorapatite: Synthesis and enhancement effect on Pb-and Cd-immobilization in polluted sediment, J. Hazard. Mater., 343 (2018) 332-339.

[36] D. Huang, W. Xue, G. Zeng, J. Wan, G. Chen, C. Huang, C. Zhang, M. Cheng, P. Xu, Immobilization of Cd in river sediments by sodium alginate modified nanoscale zero-valent iron: Impact on enzyme activities and microbial community diversity, Water Res., 106 (2016) 15-25.

[37] X. Gong, D. Huang, Y. Liu, G. Zeng, R. Wang, J. Wan, C. Zhang, M. Cheng, X. Qin, W. Xue, Stabilized nanoscale zerovalent iron mediated cadmium accumulation and oxidative damage of Boehmeria nivea (L.) Gaudich cultivated in cadmium contaminated sediments, Environ. Sci. Technol., 51 (2017) 11308-11316.

[38] B. Li, C. Lai, G. Zeng, L. Qin, H. Yi, D. Huang, C. Zhou, X. Liu, M. Cheng, P. Xu, C. Zhang, F. Huang, S. Liu, Facile Hydrothermal Synthesis of Z-scheme $Bi_2Fe_4O_9/Bi_2WO_6$ Heterojunction Photocatalyst with Enhanced Visible-Light Photocatalytic Activity, ACS Appl. Mater. Inter., (2018).

[39] L. Tang, G.M. Zeng, G.L. Shen, Y.P. Li, Y. Zhang, D.L. Huang, Rapid Detection of Picloram in Agricultural Field Samples Using a Disposable Immunomembrane-Based Electrochemical Sensor, Environ. Sci. Technol., 42 (2008) 1207-1212.

[40] J. Gong, B. Wang, G. Zeng, C. Yang, C. Niu, Q. Niu, W. Zhou, Y. Liang, Removal of cationic dyes from aqueous solution using magnetic multi-wall carbon nanotube nanocomposite as adsorbent, J. Hazard. Mater., 164 (2009) 1517-1522.

[41] P. Xu, G.M. Zeng, D.L. Huang, C.L. Feng, S. Hu, M.H. Zhao, C. Lai, Z. Wei, C. Huang, G.X. Xie, Z.F. Liu, Use of iron oxide nanomaterials in wastewater treatment: A review, Sci. Total Environ., 424 (2012) 1-10.

[42] X. Tan, Y. Liu, G. Zeng, X. Wang, X. Hu, Y. Gu, Z. Yang, Application of biochar for the removal of pollutants from aqueous solutions, Chemosphere, 125 (2015) 70-85.

[43] M. Cheng, G. Zeng, D. Huang, C. Lai, P. Xu, C. Zhang, Y. Liu, Hydroxyl radicals based advanced

oxidation processes (AOPs) for remediation of soils contaminated with organic compounds: A review, Chem. Eng. J., 284 (2016) 582-598.

[44] X. Ren, G. Zeng, L. Tang, J. Wang, J. Wan, Y. Liu, J. Yu, H. Yi, S. Ye, R. Deng, Sorption, transport and biodegradation - An insight into bioavailability of persistent organic pollutants in soil, Sci. Total Environ., 610-611 (2018) 1154-1163.

[45] C. Zhou, C. Lai, D. Huang, G. Zeng, C. Zhang, M. Cheng, L. Hu, J. Wan, W. Xiong, M. Wen, X. Wen, L. Qin, Highly porous carbon nitride by supramolecular preassembly of monomers for photocatalytic removal of sulfamethazine under visible light driven, Appl. Catal. B: Environ., 220 (2018) 202-210.

[46] F. Long, J.-L. Gong, G.-M. Zeng, L. Chen, X.-Y. Wang, J.-H. Deng, Q.-Y. Niu, H.-Y. Zhang, X.-R. Zhang, Removal of phosphate from aqueous solution by magnetic Fe-Zr binary oxide, Chem. Eng. J., 171 (2011) 448-455.

[47] M. Chen, P. Xu, G. Zeng, C. Yang, D. Huang, J. Zhang, Bioremediation of soils contaminated with polycyclic aromatic hydrocarbons, petroleum, pesticides, chlorophenols and heavy metals by composting: Applications, microbes and future research needs, Biotechnol. Adv., 33 (2015) 745-755.

[48] J.-H. Deng, X.-R. Zhang, G.-M. Zeng, J.-L. Gong, Q.-Y. Niu, J. Liang, Simultaneous removal of Cd (II) and ionic dyes from aqueous solution using magnetic graphene oxide nanocomposite as an adsorbent, Chem. Eng. J., 226 (2013) 189-200.

[49] D.-L. Huang, R.-Z. Wang, Y.-G. Liu, G.-M. Zeng, C. Lai, P. Xu, B.-A. Lu, J.-J. Xu, C. Wang, C. Huang, Application of molecularly imprinted polymers in wastewater treatment: a review, Environ. Sci. Pollut. Res. Int., 22 (2015) 963-977.

[50] C. Zhang, C. Lai, G. Zeng, D. Huang, C. Yang, Y. Wang, Y. Zhou, M. Cheng, Efficacy of carbonaceous nanocomposites for sorbing ionizable antibiotic sulfamethazine from aqueous solution, Water Res., 95 (2016) 103-112.

[51] H. Wu, C. Lai, G. Zeng, J. Liang, J. Chen, J. Xu, J. Dai, X. Li, J. Liu, M. Chen, L. Lu, L. Hu, J. Wan, The interactions of composting and biochar and their implications for soil amendment and pollution remediation: a review, Crit. Rev. Biotechnol., 37 (2017) 754-764.

[52] D. Huang, X. Wang, C. Zhang, G. Zeng, Z. Peng, J. Zhou, M. Cheng, R. Wang, Z. Hu, X. Qin, Sorptive removal of ionizable antibiotic sulfamethazine from aqueous solution by graphene oxide-coated biochar nanocomposites: Influencing factors and mechanism, Chemosphere, 186 (2017) 414-421.

[53] X. Zhang, H. Huang, J. Liu, Y. Liu, Z. Kang, Carbon quantum dots serving as spectral converters through broadband upconversion of near-infrared photons for photoelectrochemical hydrogen generation, J. Mater. Chem. A, 1 (2013) 11529-11533.

[54] Y. Zhang, G.M. Zeng, L. Tang, J. Chen, Y. Zhu, X.X. He, Y. He, Electrochemical sensor based on electrodeposited graphene-Au modified electrode and nanoAu carrier amplified signal strategy for attomolar mercury detection, Anal. Chem., 87 (2015) 989-996.

[55] D. Huang, L. Liu, G. Zeng, P. Xu, C. Huang, L. Deng, R. Wang, J. Wan, The effects of rice straw biochar on indigenous microbial community and enzymes activity in heavy metal-contaminated sediment, Chemosphere, 174 (2017) 545-553.

[56] J.K. Kim, G.D. Park, J.H. Kim, S.K. Park, Y.C. Kang, Rational Design and Synthesis of Extremely Efficient Macroporous $CoSe_2$-CNT Composite Microspheres for Hydrogen Evolution Reaction, Small, 13 (2017).

[57] Z. Sun, J. Guo, S. Zhu, L. Mao, J. Ma, D. Zhang, A high-performance Bi_2WO_6-graphene photocatalyst for visible light-induced H_2 and O_2 generation, Nanoscale, 6 (2014) 2186-2193.

[58] J. Lin, R. Zong, M. Zhou, Y. Zhu, Photoelectric catalytic degradation of methylene blue by C_{60}-modified TiO_2 nanotube array, Appl. Catal. B: Environ., 89 (2009) 425-431.

[59] G. Jiang, Z. Lin, L. Zhu, Y. Ding, H. Tang, Preparation and photoelectrocatalytic properties of titania/carbon nanotube composite films, Carbon, 48 (2010) 3369-3375.

[60] J. Liu, H. Bai, Y. Wang, Z. Liu, X. Zhang, D.D. Sun, Self-Assembling TiO_2 Nanorods on Large Graphene Oxide Sheets at a Two-Phase Interface and Their Anti-Recombination in Photocatalytic Applications, Adv. Funct. Mater., 20 (2010) 4175-4181.

[61] D.-N. Bui, S.-Z. Kang, L. Qin, X.-Q. Li, J. Mu, Relationship between the electrochemical behavior of multiwalled carbon nanotubes (MWNTs) loaded with CuO and the photocatalytic activity of Eosin Y-MWNTs-CuO system, Appl. Surf. Sci., 266 (2013) 288-293.

[62] Q. Liu, Y. Guo, Z. Chen, Z. Zhang, X. Fang, Constructing a novel ternary Fe(III)/graphene/g-C_3N_4 composite photocatalyst with enhanced visible-light driven photocatalytic activity via interfacial charge transfer effect, Appl. Catal. B: Environ., 183 (2016) 231-241.

[63] E.M. Pérez, N. Martín, π–π interactions in carbon nanostructures, Chem. Soc. Rev., 44 (2015) 6425-6433.

[64] H. Yi, G. Zeng, C. Lai, D. Huang, L. Tang, J. Gong, M. Chen, P. Xu, H. Wang, M. Cheng, C. Zhang, W. Xiong, Environment-friendly fullerene separation methods, Chem. Eng. J., 330 (2017) 134-145.

[65] S.E. Zhu, F. Li, G.W. Wang, Mechanochemistry of fullerenes and related materials, Chem. Soc. Rev., 42 (2013) 7535-7570.

[66] S.C. Smith, D.F. Rodrigues, Carbon-based nanomaterials for removal of chemical and biological contaminants from water: A review of mechanisms and applications, Carbon, 91 (2015) 122-143.

[67] M.F. De Volder, S.H. Tawfick, R.H. Baughman, A.J. Hart, Carbon nanotubes: present and future commercial applications, Science, 339 (2013) 535-539.

[68] Y. Yan, J. Miao, Z. Yang, F.X. Xiao, H.B. Yang, B. Liu, Y. Yang, Carbon nanotube catalysts: recent advances in synthesis, characterization and applications, Chem. Soc. Rev., 44 (2015) 3295-3346.

[69] X. Bai, L. Wang, Y. Wang, W. Yao, Y. Zhu, Enhanced oxidation ability of g-C_3N_4 photocatalyst via C_{60} modification, Appl. Catal. B: Environ., 152-153 (2014) 262-270.

[70] G. Li, B. Jiang, X. Li, Z. Lian, S. Xiao, J. Zhu, D. Zhang, H. Li, $C_{60}/Bi_2TiO_4F_2$ Heterojunction Photocatalysts with Enhanced Visible-Light Activity for Environmental Remediation, ACS Appl. Mater. Inter., 5 (2013) 7190-7197.

[71] H.W. Kroto, J.R. Heath, S.C. O'Brien, R.F. Curl, R.E. Smalley, C_{60}: Buckminsterfullerene, Nature, 318 (1985) 162-163.

[72] A. Hirsch, ChemInform Abstract: Principles of Fullerene Reactivity, ChemInform, 30 (2010).

[73] H. Fu, T. Xu, S. Zhu, Y. Zhu, Photocorrosion inhibition and enhancement of photocatalytic activity for ZnO via hybridization with C_{60}, Environ. Sci. Technol., 42 (2008) 8064-8069.

[74] C. García-Simón, M. Garcia-Borràs, L. Gómez, T. Parella, S. Osuna, J. Juanhuix, I. Imaz, D. Maspoch, M. Costas, X. Ribas, Sponge-like molecular cage for purification of fullerenes, Nat. Commun., 5 (2014).

[75] K.I. Guhr, M.D. Greaves, V.M. Rotello, Reversible Covalent Attachment of C_{60} to a Polymer Support, J. Am. Chem. Soc., 116 (1994) 5997-5998.

[76] C.-X. Yang, X.-P. Yan, Selective adsorption and extraction of C_{70} and higher fullerenes on a reusable metal-organic framework MIL-101(Cr), J. Mater. Chem., 22 (2012) 17833-17841.

[77] W. Krätschmer, K. Fostiropoulos, D.R. Huffman, The infrared and ultraviolet absorption spectra of laboratory-produced carbon dust: evidence for the presence of the C_{60} molecule, Chem. Phys. Lett.,

170 (1990) 167-170.

[78] L. Fulcheri, Y. Schwob, F. Fabry, G. Flamant, L.F.P. Chibante, D. Laplaze, Fullerene production in a 3-phase AC plasma process, Carbon, 38 (2000) 797-803.

[79] G.N. Churilov, W. Krätschmer, I.V. Osipova, G.A. Glushenko, N.G. Vnukova, A.L. Kolonenko, A.I. Dudnik, Synthesis of fullerenes in a high-frequency arc plasma under elevated helium pressure, Carbon, 62 (2013) 389-392.

[80] R. Doome, A. Fonseca, H. Richter, J. Nagy, P. Thiry, A. Lucas, Purification of C_{60} by fractional crystallization, J. Phys. Chem. Solids, 58 (1997) 1839-1843.

[81] M.S. Meier, J.P. Selegue, Efficient preparative separation of C_{60} and C_{70}. Gel permeation chromatography of fullerenes using 100% toluene as mobile phase, ChemInform, 23 (1992).

[82] S.B. Han, Y.H. Wei, C. Valente, I. Lagzi, J.J. Gassensmith, A. Coskun, J.F. Stoddart, B.A. Grzybowski, Chromatography in a Single Metal-Organic Framework (MOF) Crystal, J. Am. Chem. Soc., 132 (2010) 16358-16361.

[83] Q.J. Liu, N.R. Sun, M.X. Gao, C.H. Deng, Magnetic Binary Metal-Organic Framework As a Novel Affinity Probe for Highly Selective Capture of Endogenous Phosphopeptides, ACS Sustain. Chem. Eng., 6 (2018) 4382-4389.

[84] N. Bagheri, A. Khataee, B. Habibi, J. Hassanzadeh, Mimetic Ag nanoparticle/Zn-based MOF nanocomposite (AgNPs@ZnMOF) capped with molecularly imprinted polymer for the selective detection of patulin, Talanta, 179 (2018) 710-718.

[85] N. Kishi, M. Akita, M. Kamiya, S. Hayashi, H.F. Hsu, M. Yoshizawa, Facile Catch and Release of Fullerenes Using a Photoresponsive Molecular Tube, J. Am. Chem. Soc., 135 (2013) 12976-12979.

[86] N. Kishi, M. Akita, M. Yoshizawa, Selective Host-Guest Interactions of a Transformable Coordination Capsule/Tube with Fullerenes, Angew. Chem. Int. Ed., 53 (2014) 3604-3607.

[87] C.A. Hunter, K.R. Lawson, J. Perkins, C.J. Urch, Aromatic interactions, J. Chem. Soc., Perkin Trans. 2, (2001) 651-669.

[88] Y. Liu, H. Wang, P. Liang, H.-Y. Zhang, Water-Soluble Supramolecular Fullerene Assembly Mediated by Metallobridged β-Cyclodextrins, Angew. Chem. Int. Ed., 43 (2004) 2690-2694.

[89] Y. Nakanishi, H. Omachi, S. Matsuura, Y. Miyata, R. Kitaura, Y. Segawa, K. Itami, H. Shinohara, Size-Selective Complexation and Extraction of Endohedral Metallofullerenes with Cycloparaphenylene, Angew. Chem. Int. Ed., 53 (2014) 3102-3106.

[90] E.M. Pérez, L. Sánchez, G. Fernández, N. Martín, exTTF as a Building Block for Fullerene Receptors. Unexpected Solvent-Dependent Positive Homotropic Cooperativity, J. Am. Chem. Soc., 128 (2006) 7172-7173.

[91] C. García-Simón, M. Costas, X. Ribas, Metallosupramolecular receptors for fullerene binding and release, Chem. Soc. Rev., 45 (2016) 40-62.

[92] A. Ikeda, H. Udzu, M. Yoshimura, S. Shinkai, Inclusion of [60] fullerene in a self-assembled homooxacalix 3 arene-based dimeric capsule constructed by a Pd-II-pyridine interaction. The Li^+-binding to the lower rims can improve the inclusion ability, Tetrahedron, 56 (2000) 1825-1832.

[93] S. Iijima, Helical microtubules of graphitic carbon, Nature, 354 (1991) 56-58.

[94] T.W. Odom, J.L. Huang, P. Kim, C.M. Lieber, Atomic structure and electronic properties of single-walled carbon nanotubes, Nature, 391 (1998) 62-64.

[95] R.C. Haddon, Carbon nanotubes, Acc. Chem. Res., 35 (2002) 997-997.

[96] Z. Han, A. Fina, Thermal conductivity of carbon nanotubes and their polymer nanocomposites: A

review, Prog. Polym. Sci., 36 (2011) 914-944.

[97] D.S. Su, 20 Years of Carbon Nanotubes, ChemSusChem, 4 (2011) 811-813.

[98] F.R. Baptista, S.A. Belhout, S. Giordani, S.J. Quinn, Recent developments in carbon nanomaterial sensors, Chem. Soc. Rev., 44 (2015) 4433-4453.

[99] S. Kumar, R. Rani, N. Dilbaghi, K. Tankeshwar, K.-H. Kim, Carbon nanotubes: a novel material for multifaceted applications in human healthcare, Chem. Soc. Rev., 46 (2017) 158-196.

[100] Y.B. Yan, J.W. Miao, Z.H. Yang, F.X. Xiao, H.B. Yang, B. Liu, Y.H. Yang, Carbon nanotube catalysts: recent advances in synthesis, characterization and applications, Chem. Soc. Rev., 44 (2015) 3295-3346.

[101] W. Qi, X. Wang, Z. Chai, W. Hu, Low-Temperature Plasma Synthesis of Carbon Nanotubes and Graphene Based Materials and Their Fuel Cell Applications, Chem. Soc. Rev., 42 (2013) 8821-8834.

[102] I. Ibrahim, T. Gemming, W.M. Weber, T. Mikolajick, Z.F. Liu, M.H. Rummeli, Current Progress in the Chemical Vapor Deposition of Type-Selected Horizontally Aligned Single-Walled Carbon Nanotubes, ACS Nano, 10 (2016) 7248-7266.

[103] V.G. Pol, P. Thiyagarajan, Remediating plastic waste into carbon nanotubes, J. Environ. Monit., 12 (2010) 455-459.

[104] A.K. Geim, Graphene: status and prospects, Science, 324 (2009) 1530-1534.

[105] K.S. Novoselov, A.K. Geim, S. Morozov, D. Jiang, Y. Zhang, S.a. Dubonos, I. Grigorieva, A. Firsov, Electric field effect in atomically thin carbon films, Science, 306 (2004) 666-669.

[106] M.J. Allen, V.C. Tung, R.B. Kaner, Honeycomb carbon: a review of graphene, Chem. Rev., 110 (2009) 132-145.

[107] C. Chen, T. Liang, X. Chen, B. Zhang, L. Wang, J. Zhang, Phosphorus-assisted solid-phase approach to three-dimensional highly porous graphene sheets and their capacitance properties, Carbon, 132 (2018) 8-15.

[108] S. Karamat, K. Çelik, S. Shah Zaman, A. Oral, Multilayer graphene growth on polar dielectric substrates using chemical vapour deposition, Appl. Surf. Sci., 442 (2018) 720-725.

[109] P. Karaolia, I. Michael-Kordatou, E. Hapeshi, C. Drosou, Y. Bertakis, D. Christofilos, G.S. Armatas, L. Sygellou, T. Schwartz, N.P. Xekoukoulotakis, D. Fatta-Kassinos, Removal of antibiotics, antibiotic-resistant bacteria and their associated genes by graphene-based TiO_2 composite photocatalysts under solar radiation in urban wastewaters, Appl. Catal. B: Environ., 224 (2018) 810-824.

[110] Q. Guo, H. Li, Q. Zhang, Y. Zhang, Fabrication, characterization and mechanism of a novel Z-scheme Ag_3PO_4/NG/polyimide composite photocatalyst for microcystin-LR degradation, Appl. Catal. B: Environ., 229 (2018) 192-203.

[111] D.R. Dreyer, S. Park, C.W. Bielawski, R.S. Ruoff, The chemistry of graphene oxide, Chem. Soc. Rev., 39 (2010) 228-240.

[112] Y. Zhang, L.D. Li, H.Y. Liu, T.S. Lu, Graphene oxide and F co-doped TiO_2 with (001) facets for the photocatalytic reduction of bromate: Synthesis, characterization and reactivity, Chem. Eng. J., 307 (2017) 860-867.

[113] Z. Lou, M. Fujitsuka, T. Majima, Two-Dimensional Au-Nanoprism/Reduced Graphene Oxide/Pt-Nanoframe as Plasmonic Photocatalysts with Multiplasmon Modes Boosting Hot Electron Transfer for Hydrogen Generation, J. Phys. Chem. Lett., 8 (2017) 844-849.

[114] X. Zhang, L. Hou, A. Ciesielski, P. Samorì, 2D Materials Beyond Graphene for High-Performance Energy Storage Applications, Adv. Energy Mater., 6 (2016) 1600671.

[115] J.W. May, Platinum surface LEED rings, Surf. Sci., 17 (1969) 267-270.

[116] X.K. Lu, M.F. Yu, H. Huang, R.S. Ruoff, Tailoring graphite with the goal of achieving single sheets, Nanotechnology, 10 (1999) 269-272.

[117] B. He, Y. Yang, M.F. Yuen, X.F. Chen, C.S. Lee, W.J. Zhang, Vertical nanostructure arrays by plasma etching for applications in biology, energy, and electronics, Nano Today, 8 (2013) 265-289.

[118] K.S. Kim, Y.J. Ji, Y. Nam, K.H. Kim, E. Singh, J.Y. Lee, G.Y. Yeom, Atomic layer etching of graphene through controlled ion beam for graphene-based electronics, Sci. Rep., 7 (2017).

[119] K.-Q. Lu, L. Yuan, X. Xin, Y.-J. Xu, Hybridization of graphene oxide with commercial graphene for constructing 3D metal-free aerogel with enhanced photocatalysis, Appl. Catal. B: Environ., 226 (2018) 16-22.

[120] W.D. Tennyson, M. Tian, A.B. Papandrew, C.M. Rouleau, A.A. Puretzky, B.T. Sneed, K.L. More, G.M. Veith, G. Duscher, T.A. Zawodzinski, Bottom up synthesis of boron-doped graphene for stable intermediate temperature fuel cell electrodes, Carbon, 123 (2017) 605-615.

[121] V.P. Pham, H.S. Jang, D. Whang, J.Y. Choi, Direct growth of graphene on rigid and flexible substrates: progress, applications, and challenges, Chem. Soc. Rev., 46 (2017) 6276-6300.

[122] S. Kim, J.K. Seo, J.H. Park, Y. Song, Y.S. Meng, M.J. Heller, White-light emission of blue-luminescent graphene quantum dots by europium (III) complex incorporation, Carbon, 124 (2017) 479-485.

[123] E.F. Talantsev, W.P. Crump, J.L. Tallon, Two-band induced superconductivity in single-layer graphene and topological insulator bismuth selenide, Supercond. Sci. Technol., 31 (2018) 015011.

[124] C.K. Chua, M. Pumera, Chemical reduction of graphene oxide: a synthetic chemistry viewpoint, Chem. Soc. Rev., 43 (2014) 291-312.

[125] H. Sun, S. Liu, G. Zhou, H.M. Ang, M.O. Tadé, S. Wang, Reduced Graphene Oxide for Catalytic Oxidation of Aqueous Organic Pollutants, ACS Appl. Mater. Inter., 4 (2012) 5466-5471.

[126] Y. Wang, H. Cao, L. Chen, C. Chen, X. Duan, Y. Xie, W. Song, H. Sun, S. Wang, Tailored synthesis of active reduced graphene oxides from waste graphite: Structural defects and pollutant-dependent reactive radicals in aqueous organics decontamination, Appl. Catal. B: Environ., 229 (2018) 71-80.

[127] C.M. Park, J. Heo, D.L. Wang, C.M. Su, Y. Yoon, Heterogeneous activation of persulfate by reduced graphene oxide-elemental silver/magnetite nanohybrids for the oxidative degradation of pharmaceuticals and endocrine disrupting compounds in water, Appl. Catal. B: Environ., 225 (2018) 91-99.

[128] M.M. El-Wekil, A.M. Mahmoud, S.A. Alkahtani, A.A. Marzouk, R. Ali, A facile synthesis of 3D $NiFe_2O_4$ nanospheres anchored on a novel ionic liquid modified reduced graphene oxide for electrochemical sensing of ledipasvir: Application to human pharmacokinetic study, Biosens. Bioelectron., 109 (2018) 164-170.

[129] R.S. Dey, S. Hajra, R.K. Sahu, C.R. Raj, M.K. Panigrahi, A rapid room temperature chemical route for the synthesis of graphene: metal-mediated reduction of graphene oxide, Chem. Commun., 48 (2012) 1787-1789.

[130] V. Chabot, D. Higgins, A. Yu, X. Xiao, Z. Chen, J. Zhang, A review of graphene and graphene oxide sponge: material synthesis and applications to energy and the environment, Energy Environ. Sci., 7 (2014) 1564-1596.

[131] A. Dasgupta, L.P. Rajukumar, C. Rotella, Y. Lei, M. Terrones, Covalent three-dimensional networks of graphene and carbon nanotubes: synthesis and environmental applications, Nano Today, 12 (2017)

116-135.

[132] S. Nardecchia, D. Carriazo, M.L. Ferrer, M.C. Gutiérrez, F. del Monte, Three dimensional macroporous architectures and aerogels built of carbon nanotubes and/or graphene: synthesis and applications, Chem. Soc. Rev., 42 (2013) 794-830.

[133] T. Liu, M. Huang, X. Li, C. Wang, C.-X. Gui, Z.-Z. Yu, Highly compressible anisotropic graphene aerogels fabricated by directional freezing for efficient absorption of organic liquids, Carbon, 100 (2016) 456-464.

[134] X. Du, H.-Y. Liu, Y.-W. Mai, Ultrafast synthesis of multifunctional N-doped graphene foam in an ethanol flame, ACS Nano, 10 (2015) 453-462.

[135] K. Goh, W. Jiang, H.E. Karahan, S. Zhai, L. Wei, D. Yu, A.G. Fane, R. Wang, Y. Chen, All-carbon nanoarchitectures as high-performance separation membranes with superior stability, Adv. Funct. Mater., 25 (2015) 7348-7359.

[136] Y.P. Wu, N.B. Yi, L. Huang, T.F. Zhang, S.L. Fang, H.C. Chang, N. Li, J. Oh, J.A. Lee, M. Kozlov, A.C. Chipara, H. Terrones, P. Xiao, G.K. Long, Y. Huang, F. Zhang, L. Zhang, X. Lepro, C. Haines, M.D. Lima, N.P. Lopez, L.P. Rajukumar, A.L. Elias, S.M. Feng, S.J. Kim, N.T. Narayanan, P.M. Ajayan, M. Terrones, A. Aliev, P.F. Chu, Z. Zhang, R.H. Baughman, Y.S. Chen, Three-dimensionally bonded spongy graphene material with super compressive elasticity and near-zero Poisson's ratio, Nat. Commun., 6 (2015).

[137] X.L. Zou, L.Q. Wang, B.I. Yakobson, Mechanisms of the oxygen reduction reaction on B- and/or N-doped carbon nanomaterials with curvature and edge effects, Nanoscale, 10 (2018) 1129-1134.

[138] C. Lai, M.-M. Wang, G.-M. Zeng, Y.-G. Liu, D.-L. Huang, C. Zhang, R.-Z. Wang, P. Xu, M. Cheng, C. Huang, H.-P. Wu, L. Qin, Synthesis of surface molecular imprinted TiO_2/graphene photocatalyst and its highly efficient photocatalytic degradation of target pollutant under visible light irradiation, Appl. Surf. Sci., 390 (2016) 368-376.

[139] J. Wang, L. Tang, G. Zeng, Y. Deng, H. Dong, Y. Liu, L. Wang, B. Peng, C. Zhang, F. Chen, 0D/2D interface engineering of carbon quantum dots modified Bi_2WO_6 ultrathin nanosheets with enhanced photoactivity for full spectrum light utilization and mechanism insight, Appl. Catal. B: Environ., 222 (2018) 115-123.

[140] J. Zhang, Z.-H. Huang, Y. Xu, F. Kang, Hydrothermal Synthesis of Graphene/Bi_2WO_6 Composite with High Adsorptivity and Photoactivity for Azo Dyes, J. Am. Ceram. Soc., 96 (2013) 1562-1569.

[141] R. Wang, K.-Q. Lu, F. Zhang, Z.-R. Tang, Y.-J. Xu, 3D carbon quantum dots/graphene aerogel as a metal-free catalyst for enhanced photosensitization efficiency, Appl. Catal. B: Environ., 233 (2018) 11-18.

[142] X. Zhao, H. Liu, Y. Shen, J. Qu, Photocatalytic reduction of bromate at C_{60} modified Bi_2MoO_6 under visible light irradiation, Appl. Catal. B: Environ., 106 (2011) 63-68.

[143] L. Yu, S. Ruan, X. Xu, R. Zou, J. Hu, One-dimensional nanomaterial-assembled macroscopic membranes for water treatment, Nano Today, (2017).

[144] J. Di, J. Xia, Y. Ge, H. Li, H. Ji, H. Xu, Q. Zhang, H. Li, M. Li, Novel visible-light-driven CQDs/Bi_2WO_6 hybrid materials with enhanced photocatalytic activity toward organic pollutants degradation and mechanism insight, Appl. Catal. B: Environ., 168 (2015) 51-61.

[145] F.-Y. Liu, Y.-R. Jiang, C.-C. Chen, W.W. Lee, Novel synthesis of $PbBiO_2Cl$/BiOCl nanocomposite with enhanced visible-driven-light photocatalytic activity, Catal. Today, 300 (2018) 112-123.

[146] H. He, L. Huang, Z. Zhong, S. Tan, Constructing three-dimensional porous graphene-carbon quantum dots/g-C_3N_4 nanosheet aerogel metal-free photocatalyst with enhanced photocatalytic

activity, Appl. Surf. Sci., 441 (2018) 285-294.

[147] X. Zhang, S. Cao, Z. Wu, S. Zhao, L. Piao, Enhanced photocatalytic activity towards degradation and H_2 evolution over one dimensional TiO_2@MWCNTs heterojunction, Appl. Surf. Sci., 402 (2017) 360-368.

[148] E. Gao, W. Wang, M. Shang, J. Xu, Synthesis and enhanced photocatalytic performance of graphene-Bi_2WO_6 composite, Phys. Chem. Chem. Phys., 13 (2011) 2887-2893.

[149] J. Yang, X.X. Shen, Y.J. Li, L.Y. Bian, J. Dai, D.S. Yuan, Bismuth Tungstate-Reduced Graphene Oxide Self-Assembled Nanocomposites for the Selective Photocatalytic Oxidation of Alcohols in Water, Chemcatchem, 8 (2016) 1399-1409.

[150] E.T. Martin, C.M. McGuire, M.S. Mubarak, D.G. Peters, Electroreductive Remediation of Halogenated Environmental Pollutants, Chem. Rev., 116 (2016) 15198-15234.

[151] L. Ju, P. Wu, X. Lai, S. Yang, B. Gong, M. Chen, N. Zhu, Synthesis and characterization of Fullerene modified ZnAlTi-LDO in photo-degradation of Bisphenol A under simulated visible light irradiation, Environ. Pollut., 228 (2017) 234-244.

[152] G.L.M. Leonard, S. Remy, B. Heinrichs, Doping TiO_2 films with carbon nanotubes to simultaneously optimise antistatic, photocatalytic and superhydrophilic properties, J. Sol-Gel Sci. Technol., 79 (2016) 413-425.

[153] Y.-P. Sun, B. Zhou, Y. Lin, W. Wang, K.S. Fernando, P. Pathak, M.J. Meziani, B.A. Harruff, X. Wang, H. Wang, Quantum-sized carbon dots for bright and colorful photoluminescence, J. Am. Chem. Soc, 128 (2006) 7756-7757.

[154] X. Wu, J. Zhao, S. Guo, L. Wang, W. Shi, H. Huang, Y. Liu, Z. Kang, Carbon dot and $BiVO_4$ quantum dot composites for overall water splitting via a two-electron pathway, Nanoscale, 8 (2016) 17314-17321.

[155] S.Y. Lim, W. Shen, Z. Gao, Carbon quantum dots and their applications, Chem. Soc. Rev., 44 (2015) 362-381.

[156] P. Mirtchev, E.J. Henderson, N. Soheilnia, C.M. Yip, G.A. Ozin, Solution phase synthesis of carbon quantum dots as sensitizers for nanocrystalline TiO_2 solar cells, J. Mater. Chem., 22 (2012) 1265-1269.

[157] H. Zhang, H. Huang, H. Ming, H. Li, L. Zhang, Y. Liu, Z. Kang, Carbon quantum dots/Ag_3PO_4 complex photocatalysts with enhanced photocatalytic activity and stability under visible light, J. Mater. Chem., 22 (2012) 10501-10506.

[158] F. Nan, Z. Kang, J. Wang, M. Shen, L. Fang, Carbon quantum dots coated $BiVO_4$ inverse opals for enhanced photoelectrochemical hydrogen generation, Appl. Phys. Lett., 106 (2015).

[159] L. Xu, J. Sun, Recent Advances in the Synthesis and Application of Two-Dimensional Zeolites, Adv. Energy Mater., 6 (2016).

[160] S. Kim, M. Kim, Y.K. Kim, S.-H. Hwang, S.K. Lim, Core-shell-structured carbon nanofiber-titanate nanotubes with enhanced photocatalytic activity, Appl. Catal. B: Environ., 148 (2014) 170-176.

[161] M. Zhu, Y. Muhammad, P. Hu, B. Wang, Y. Wu, X. Sun, Z. Tong, Z. Zhao, Enhanced interfacial contact of dopamine bridged melamine-graphene/TiO_2 nano-capsules for efficient photocatalytic degradation of gaseous formaldehyde, Appl. Catal. B: Environ., 232 (2018) 182-193.

[162] J. Li, X. Wang, G. Zhao, C. Chen, Z. Chai, A. Alsaedi, T. Hayat, X. Wang, Metal-organic framework-based materials: superior adsorbents for the capture of toxic and radioactive metal ions, Chem. Soc. Rev., 47 (2018) 2322-2356.

[163] Y. Zhou, X.J. Zhang, Q. Zhang, F. Dong, F. Wang, Z. Xiong, Role of graphene on the band structure

and interfacial interaction of Bi_2WO_6/graphene composites with enhanced photocatalytic oxidation of NO, J. Mater. Chem. A, 2 (2014) 16623-16631.

[164] J. Sun, J. Zhang, H. Fu, H. Wan, Y. Wan, X. Qu, Z. Xu, D. Yin, S. Zheng, Enhanced catalytic hydrogenation reduction of bromate on Pd catalyst supported on CeO_2 modified SBA-15 prepared by strong electrostatic adsorption, Appl. Catal. B: Environ., 229 (2018) 32-40.

[165] F. Chen, Q. Yang, Y. Zhong, H. An, J. Zhao, T. Xie, Q. Xu, X. Li, D. Wang, G. Zeng, Photo-reduction of bromate in drinking water by metallic Ag and reduced graphene oxide (RGO) jointly modified BiVO4 under visible light irradiation, Water Res., 101 (2016) 555-563.

[166] W.G. Tu, Y. Zhou, Z.G. Zou, Versatile Graphene-Promoting Photocatalytic Performance of Semiconductors: Basic Principles, Synthesis, Solar Energy Conversion, and Environmental Applications, Adv. Funct. Mater., 23 (2013) 4996-5008.

[167] P. Dong, G. Hou, X. Xi, R. Shao, F. Dong, WO3-based photocatalysts: morphology control, activity enhancement and multifunctional applications, Environ. Sci. Nano, 4 (2017) 539-557.

[168] J. Wu, B. Liu, Z. Ren, M. Ni, C. Li, Y. Gong, W. Qin, Y. Huang, C.Q. Sun, X. Liu, CuS/RGO hybrid photocatalyst for full solar spectrum photoreduction from UV/Vis to near-infrared light, J. Colloid Interface Sci., 517 (2018) 80-85.

[169] Y.-J. Yuan, D.-Q. Chen, X.-F. Shi, J.-R. Tu, B. Hu, L.-X. Yang, Z.-T. Yu, Z.-G. Zou, Facile fabrication of “green” SnS_2 quantum dots/reduced graphene oxide composites with enhanced photocatalytic performance, Chem. Eng. J., 313 (2017) 1438-1446.

[170] L. Cai, X. Xiong, N. Liang, Q. Long, Highly effective and stable Ag_3PO_4–WO_3/MWCNTs photocatalysts for simultaneous Cr(VI) reduction and orange II degradation under visible light irradiation, Appl. Surf. Sci., 353 (2015) 939-948.

[171] Y. Li, Z. Liu, Y. Wu, J. Chen, J. Zhao, F. Jin, P. Na, Carbon dots-TiO_2 nanosheets composites for photoreduction of Cr(VI) under sunlight illumination: Favorable role of carbon dots, Appl. Catal. B: Environ., 224 (2018) 508-517.

[172] X.K. Zeng, G. Wang, Y. Liu, X.W. Zhang, Graphene-based antimicrobial nanomaterials: rational design and applications for water disinfection and microbial control, Environ. Sci. Nano, 4 (2017) 2248-2266.

[173] X. Zeng, Z. Wang, G. Wang, T.R. Gengenbach, D.T. McCarthy, A. Deletic, J. Yu, X. Zhang, Highly dispersed TiO_2 nanocrystals and WO_3 nanorods on reduced graphene oxide: Z-scheme photocatalysis system for accelerated photocatalytic water disinfection, Appl. Catal. B: Environ., 218 (2017) 163-173.

[174] C. Sichel, M. de Cara, J. Tello, J. Blanco, P. Fernandez-Ibanez, Solar photocatalytic disinfection of agricultural pathogenic fungi: Fusarium species, Appl. Catal. B: Environ., 74 (2007) 152-160.

[175] X. Zeng, Z. Wang, N. Meng, D.T. McCarthy, A. Deletic, J.-h. Pan, X. Zhang, Highly dispersed TiO_2 nanocrystals and carbon dots on reduced graphene oxide: Ternary nanocomposites for accelerated photocatalytic water disinfection, Appl. Catal. B: Environ., 202 (2017) 33-41.

[176] B.R. Cruz-Ortiz, J.W.J. Hamilton, C. Pablos, L. Díaz-Jiménez, D.A. Cortés-Hernández, P.K. Sharma, M. Castro-Alférez, P. Fernández-Ibañez, P.S.M. Dunlop, J.A. Byrne, Mechanism of photocatalytic disinfection using titania-graphene composites under UV and visible irradiation, Chem. Eng. J., 316 (2017) 179-186.

[177] C.-H. Deng, J.-L. Gong, G.-M. Zeng, Y. Jiang, C. Zhang, H.-Y. Liu, S.-Y. Huan, Graphene-CdS nanocomposite inactivation performance toward Escherichia coli in the presence of humic acid under visible light irradiation, Chem. Eng. J., 284 (2016) 41-53.

[178] G.H. Moon, W. Kim, A.D. Bokare, N.E. Sung, W. Choi, Solar production of H_2O_2 on reduced graphene oxide-TiO_2 hybrid photocatalysts consisting of earth-abundant elements only, Energy Environ. Sci., 7 (2014) 4023-4028.

[179] S. Cao, C. Chen, J. Zhang, C. Zhang, W. Yu, B. Liang, Y. Tsang, MnOx quantum dots decorated reduced graphene oxide/TiO_2 nanohybrids for enhanced activity by a UV pre-catalytic microwave method, Appl. Catal. B: Environ., 176-177 (2015) 500-512.

[180] V. Georgakilas, A. Demeslis, E. Ntararas, A. Kouloumpis, K. Dimos, D. Gournis, M. Kocman, M. Otyepka, R. Zbořil, Hydrophilic nanotube supported graphene-water dispersible carbon superstructure with excellent conductivity, Adv. Funct. Mater., 25 (2015) 1481-1487.

[181] D. Liu, J. Ma, R. Long, C. Gao, Y. Xiong, Silicon nanostructures for solar-driven catalytic applications, Nano Today, (2017).

[182] Z. Kou, B. Guo, Y. Zhao, S. Huang, T. Meng, J. Zhang, W. Li, I.S. Amiinu, Z. Pu, M. Wang, Molybdenum carbide-derived chlorine-doped ordered mesoporous carbon with few-layered graphene walls for energy storage applications, ACS Appl. Mater. Inter., 9 (2017) 3702-3712.

[183] M. Lozada-Hidalgo, S. Zhang, S. Hu, V.G. Kravets, F.J. Rodriguez, A. Berdyugin, A. Grigorenko, A.K. Geim, Giant photoeffect in proton transport through graphene membranes, Nat Nanotechnol, 13 (2018) 300-303.

[184] S. Zhang, L. Wang, C. Liu, J. Luo, J. Crittenden, X. Liu, T. Cai, J. Yuan, Y. Pei, Y. Liu, Photocatalytic wastewater purification with simultaneous hydrogen production using MoS_2 QD-decorated hierarchical assembly of $ZnIn_2S_4$ on reduced graphene oxide photocatalyst, Water Res., 121 (2017) 11-19.

[185] Y. Yan, B. Xia, Z. Xu, X. Wang, Recent development of molybdenum sulfides as advanced electrocatalysts for hydrogen evolution reaction, ACS Catal., 4 (2014) 1693-1705.

[186] H. Nolan, N. McEvoy, M. O'Brien, N.C. Berner, C. Yim, T. Hallam, A.R. McDonald, G.S. Duesberg, Molybdenum disulfide/pyrolytic carbon hybrid electrodes for scalable hydrogen evolution, Nanoscale, 6 (2014) 8185-8191.

[187] Y. Han, H. Huang, H. Zhang, Y. Liu, X. Han, R. Liu, H. Li, Z. Kang, Carbon quantum dots with photoenhanced hydrogen-bond catalytic activity in aldol condensations, ACS Catal., 4 (2014) 781-787.

[188] S. Zhao, C. Li, J. Liu, N. Liu, S. Qiao, Y. Han, H. Huang, Y. Liu, Z. Kang, Carbon quantum dots/SnO_2-Co_3O_4 composite for highly efficient electrochemical water oxidation, Carbon, 92 (2015) 64-73.

[189] S. Zhao, C. Li, L. Wang, N. Liu, S. Qiao, B. Liu, H. Huang, Y. Liu, Z. Kang, Carbon quantum dots modified MoS_2 with visible-light-induced high hydrogen evolution catalytic ability, Carbon, 99 (2016) 599-606.

[190] Y. Chen, G. Tian, Z. Ren, K. Pan, Y. Shi, J. Wang, H. Fu, Hierarchical Core-Shell Carbon Nanofiber@$ZnIn_2S_4$ Composites for Enhanced Hydrogen Evolution Performance, ACS Appl. Mater. Inter., 6 (2014) 13841-13849.

[191] Z. Li, B. Tian, W. Zhen, Y. Wu, G. Lu, Inhibition of hydrogen and oxygen recombination using oxygen transfer reagent hemin chloride in Pt/TiO_2 dispersion for photocatalytic hydrogen generation, Appl. Catal. B: Environ., 203 (2017) 408-415.

[192] L. Li, Z. Cai, Q. Wu, W.-Y. Lo, N. Zhang, L.X. Chen, L. Yu, Rational Design of Porous Conjugated Polymers and Roles of Residual Palladium for Photocatalytic Hydrogen Production, J. Am. Chem. Soc., 138 (2016) 7681-7686.

[193] Y. Yang, C. Zhang, C. Lai, G. Zeng, D. Huang, M. Cheng, J. Wang, F. Chen, C. Zhou, W. Xiong, BiOX (X = Cl, Br, I) photocatalytic nanomaterials: Applications for fuels and environmental management, Adv. Colloid Interface Sci., 254 (2018) 76-93.

[194] A. Kouloumpis, N. Vourdas, P. Zygouri, N. Chalmpes, G. Potsi, V. Kostas, K. Spyrou, V.N. Stathopoulos, D. Gournis, P. Rudolf, Controlled deposition of fullerene derivatives within a graphene template by means of a modified Langmuir-Schaefer method, J. Colloid Interface Sci., 524 (2018) 388-398.

[195] K.Q. Lu, L. Yuan, X. Xin, Y.J. Xu, Hybridization of graphene oxide with commercial graphene for constructing 3D metal-free aerogel with enhanced photocatalysis, Appl. Catal. B: Environ., 226 (2018) 16-22.

[196] L. Zhao, X.L. Sui, J.Z. Li, J.J. Zhang, L.M. Zhang, G.S. Huang, Z.B. Wang, Supramolecular assembly promoted synthesis of three-dimensional nitrogen doped graphene frameworks as efficient electrocatalyst for oxygen reduction reaction and methanol electrooxidation, Appl. Catal. B: Environ., 231 (2018) 224-233.

[197] J. Liu, M. Durstock, L. Dai, Graphene oxide derivatives as hole- and electron-extraction layers for high-performance polymer solar cells, Energy Environ. Sci., 7 (2014) 1297-1306.

[198] E. Istif, J. Hernandez-Ferrer, E.P. Urriolabeitia, A. Stergiou, N. Tagmatarchis, G. Fratta, M.J. Large, A.B. Dalton, A.M. Benito, W.K. Maser, Conjugated Polymer Nanoparticle-Graphene Oxide Charge-Transfer Complexes, Adv. Funct. Mater., 28 (2018).

[199] E. Jokar, Z.Y. Huang, S. Narra, C.Y. Wang, V. Kattoor, C.C. Chung, E.W.G. Diau, Anomalous Charge-Extraction Behavior for Graphene-Oxide (GO) and Reduced Graphene-Oxide (rGO) Films as Efficient p-Contact Layers for High-Performance Perovskite Solar Cells, Adv. Energy Mater., 8 (2018).